

Enumeration of Hybrid Domino-Lozenge Tilings III: Centrally Symmetric Tilings

Tri Lai

Department of Mathematics
University of Nebraska – Lincoln
Lincoln, NE 68588-0130
tlai3@unl.edu

Mathematics Subject Classifications: 05A15, 05B45, 05C50

Abstract

We use the subgraph replacement method to investigate new properties of the tilings of regions on the square lattice with diagonals drawn in. In particular, we show that the centrally symmetric tilings of a generalization of the Aztec diamond are always enumerated by a simple product formula. This result generalizes the previous work of M. Ciucu and B.-Y. Yang about symmetric tilings of the Aztec diamond. We also use our method to prove a closed form product formula for the number of centrally symmetric tilings of a quasi-hexagon.

Keywords: perfect matchings, hybrid domino-lozenge tilings, dual graph, subgraph replacement.

1 Introduction

The hybrid domino-lozenge tilings drawn in was first studied by J. Propp in the 1990s (see [19] and the list of references therein). In 1996, C. Douglas [7] proved a conjecture posed by J. Propp about the number of tilings of an analog of the Aztec diamond on the square lattice with every second diagonal¹ drawn in (see Figure 1.1 for several first regions of Douglas). In particular, Douglas showed that the region of order n has exactly $2^{n(n+1)}$ tilings.

Recently, the author [17, 18] generalized Douglas’ theorem and the Aztec diamond theorem by N. Elkies, G. Kuperberg, M. Larsen, and J. Propp [8, 9] by enumerating tilings of a family of 4-sided regions on the square lattice with arbitrary diagonals drawn in (see Figure 1.2 for an example of the region). We call this region a *generalized Douglas region* (or simply a *Douglas region* in this paper). In particular, we showed that the tiling number of a Douglas region is always given by a power of 2 (see Theorem 4 in [17]). This implies Douglas’ theorem when the distances between any two consecutive diagonals are all $2\sqrt{2}$, and the Aztec diamond theorem when there are no drawn-in diagonal.

Propp [19] also investigated a ‘natural hybrid’ between the Aztec diamond and a lozenge hexagon on the square lattice with every third diagonal drawn in, called a *quasi-hexagon*. Finding an explicit tiling formula for a quasi-hexagon was a long-standing open problem in the field (see Problem 16 on Propp’s well-known list of 32 open problems in enumeration of tilings [19]). The author [13] solved this problem by using the subgraph replacement method. In general, there is no simple product formula for the number of tilings of a quasi-hexagon. However, in the symmetric case, we have a simple product formula, which is a certain product of a power of 2 and an instance of MacMahon’s tiling formula for a semi-regular hexagon on the triangular lattice [11]. The author [15] also enumerated tiling of an 8-vertex counter part of the quasi-hexagons, called *quasi-octagons*.

¹From now on, we use the word “diagonal” to mean “southwest-to-northeast diagonal”

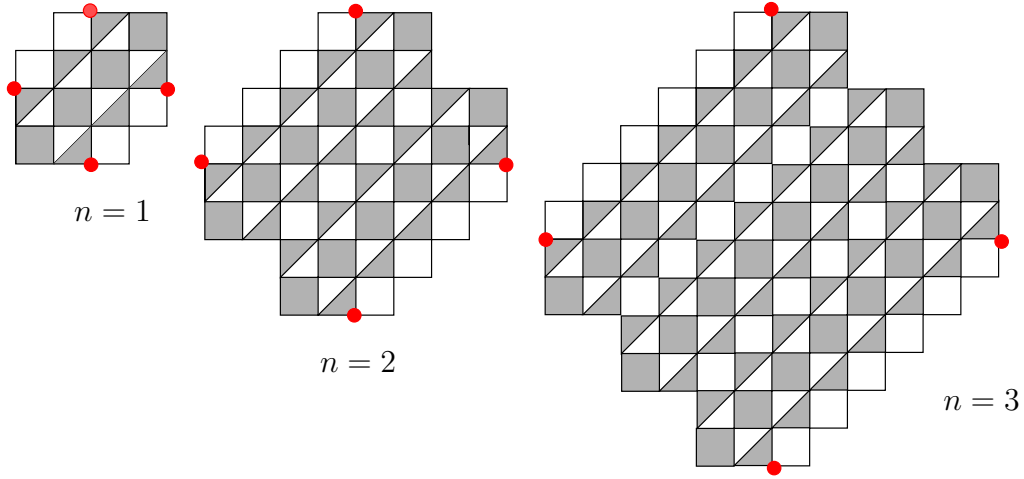


Figure 1.1: The (original) Douglas regions of order $n = 1$, $n = 2$ and $n = 3$. The figure was first introduced in [13].

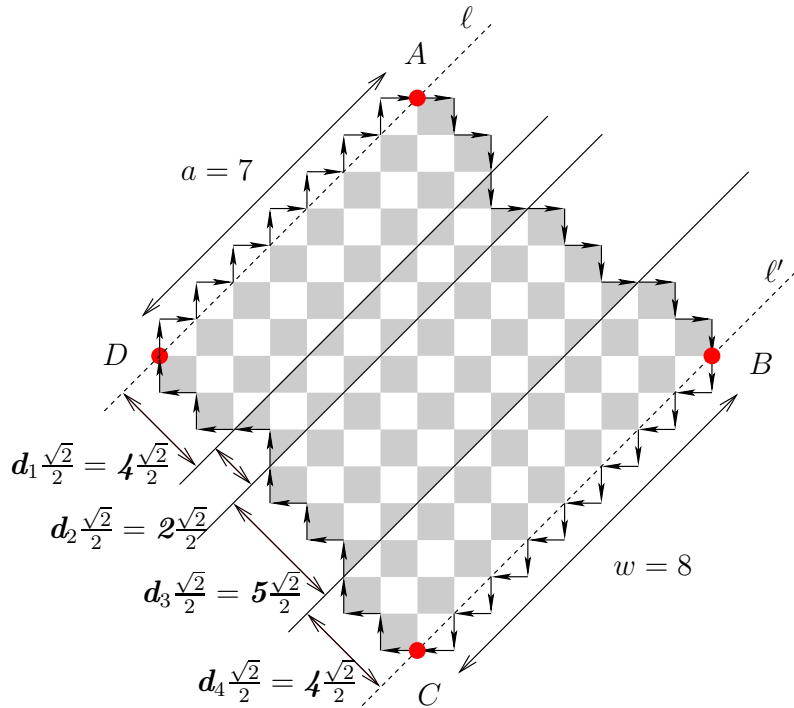


Figure 1.2: The Douglas region $\mathcal{D}_7(4, 2, 5, 4)$. The figure was first introduced in [17].

Inspired by the work of B.Y. Yang [22] and M. Ciucu [2] on the symmetric tilings of the Aztec diamond, we consider the *centrally symmetric tilings* (i.e. the tilings which are invariant under the 180° rotation) of a Douglas region. We actually investigate a more general case when certain portions of the region have been removed along a symmetry axis as in Figure 2.2 (the black parts indicate the removed portions). We show that the number of centrally symmetric tilings of such a Douglas region with ‘defects’ is always given by a closed form product formula (see Theorem 2.1 in Section 2).

The study of symmetric (lozenge) tilings of a hexagon on the triangular lattice dates back to the late 1890s when MacMahon conjectured the q -enumeration of the symmetric plane partitions [12]. About one hundred years later, all 10 symmetry classes of plane partitions were collected in Stanley’s classical papers [20]. Each of these symmetry classes can be translated into a certain class of symmetric tilings of a hexagon. As one of the 10 symmetry classes, the *self-complementary plane partitions* correspond to the centrally symmetric tilings of a hexagon. Stanley [20] showed that the number of self-complementary plane partitions, and hence the number of centrally symmetric tilings of a hexagon, is a simple product formula. Viewing a quasi-hexagon as a generalization of a normal hexagon, we now investigate centrally symmetric tilings of quasi-hexagons. In particular, use the subgraph replacement method to show that the number of centrally symmetric tilings of a quasi-hexagon is also given by a simple product formula (see Theorem 2.2 in Section 2).

The rest of this paper is organized as follows. We give detailed definitions of the Douglas regions and the quasi-hexagons, and the statement of our main results (Theorems 2.1 and 2.2) in Section 2. Section 3 is devoted to several fundamental results in the subgraph replacement method that will be employed in our proofs. In Section 4, we enumerate the perfect matchings of an Aztec rectangle graph with holes, that itself can be considered as a generalization of the related work of B.Y. Yang [22] and M. Ciucu [2] in the case of the Aztec diamonds. We will use this enumeration in our proof of Theorem 2.1 in Section 5. Finally, in Section 6, we present the proof of Theorem 2.2.

2 Statement of the main results

A lattice divides the plane into disjoint fundamental regions, called *cells*. A (lattice) *region* is a finite connected union of cells. A *tile* is the union of any two cells sharing an edge. A *tiling* of a region \mathcal{R} is a covering of \mathcal{R} by tiles so that there are no gaps or overlaps. The number of tilings of the region \mathcal{R} is denoted by $M(\mathcal{R})$.

Let ℓ be a fixed drawn-in diagonal on the square lattice. Assume that k more diagonals have been drawn in above ℓ with the distances between two consecutive ones from the top $d_1 \frac{\sqrt{2}}{2}, d_2 \frac{\sqrt{2}}{2}, \dots, d_k \frac{\sqrt{2}}{2}$, and k' more diagonals have been drawn in below ℓ with the distances between two consecutive ones from the bottom $d'_1 \frac{\sqrt{2}}{2}, d'_2 \frac{\sqrt{2}}{2}, \dots, d'_{k'} \frac{\sqrt{2}}{2}$ (see Figure 2.1). Next, we color black and white the dissection obtained from the above set-up of drawn-in diagonals on the square lattice, so that two cells sharing an edge have different colors.

We define the *quasi-hexagon* $\mathcal{H}_a(d_1, d_2, \dots, d_k; d'_1, d'_2, \dots, d'_{k'})$ as follows. Pick a lattice point A on the top drawn-in diagonal. Start from A we go south or west in each step so that the black cell stays on the left. The resulting lattice path from A intersects the diagonal ℓ at a lattice point B . From B , we go south or west so that the white cell stays on the left in each step. Our lattice path stops when reaching the bottom drawn-in diagonal at a lattice point C . The described lattice path passing A , B and C is the southwestern boundary of the region. Next, we pick a lattice point F on the top drawn-in diagonal so that F is $a\sqrt{2}$ units on the right of A . The northeastern boundary is obtained from the southwestern one by reflecting about the perpendicular bisector of the segment AF and changing the steps from south to north and from west to east. Assume that the northeastern boundary intersects ℓ and the bottom drawn-in diagonal by E and D , respectively. We complete the boundary of the region by connecting C and D , and F and A along the drawn-in diagonal. The six lattice points A, B, C, D, E , and F are called the *vertices* of the region, and the diagonal ℓ are called the (southwest-to-northeast) axis of the region.

The cells in a quasi-hexagon are unit squares or triangles. The triangular cells only appear along the drawn-in diagonals. A *row of cells* consists of all the triangular cells of a given color with bases resting

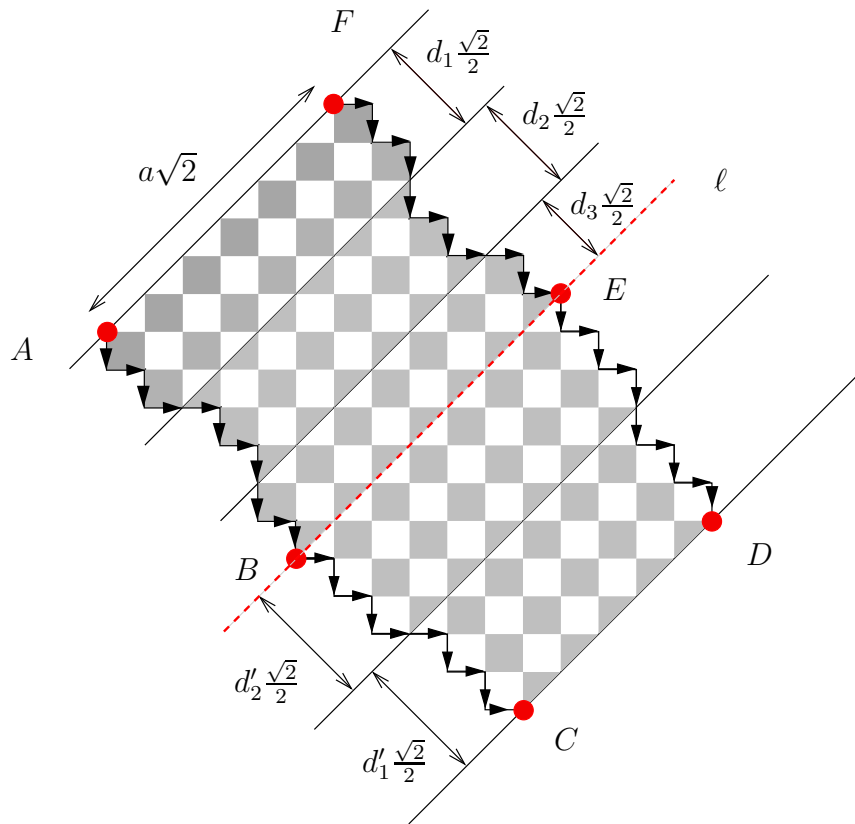


Figure 2.1: The quasi-hexagon $\mathcal{H}_6(4, 4, 3; 5, 5)$. The figure first appeared in [13].

on a fixed lattice diagonal, or consists of all the square cells² (of a given color) passed through by a fixed lattice diagonal.

Define the (*generalized*) *Douglas region* $\mathcal{D}_a(d_1, \dots, d_k)$ to be the region obtained from the portion of $\mathcal{H}_a(d_1, \dots, d_k; d'_1, \dots, d'_{k'})$ above the axis ℓ by replacing the triangles running along the top and the bottom by squares of the same color (see Figure 1.2). The (*generalized*) Douglas region was first investigated in [13], and also in [17] and [18] as a common generalization of the original Douglas regions [7] and the Aztec diamonds [8, 9].

Remark 1. As mentioned in [13] (Theorem 2.1(a) and Theorem 2.3(a)), if the triangles running along the bottom of a quasi-hexagon or a Douglas region are black, then the region has no tilings. *Therefore, from now on, we assume that the bottom triangles are white.* This is equivalent to the fact that the last step of the southwestern boundary is an east step.

For any finite set of integers $A = \{a_1, a_2, \dots, a_n\}$, $n \geq 0$, we define four functions

$$E(a_1, a_2, \dots, a_n) = \frac{2^{n^2}}{0!2!4! \dots (2n-2)!} \prod_{1 \leq i < j \leq n} (a_j - a_i) \prod_{1 \leq i < j \leq n} (a_i + a_j - 1), \quad (2.1)$$

$$O(a_1, a_2, \dots, a_n) = \frac{2^{n^2}}{1!3!5! \dots (2n-1)!} \prod_{1 \leq i < j \leq n} (a_j - a_i) \prod_{1 \leq i < j \leq n} (a_i + a_j - 1), \quad (2.2)$$

$$\bar{E}(a_1, a_2, \dots, a_n) = \frac{2^{n^2} \prod_{i=1}^n a_i}{0!2!4! \dots (2n-2)!} \prod_{1 \leq i < j \leq n} (a_j - a_i) \prod_{1 \leq i < j \leq n} (a_i + a_j), \quad (2.3)$$

and

$$\bar{O}(a_1, a_2, \dots, a_n) = \frac{2^{n^2} \prod_{i=1}^n a_i}{1!3!5! \dots (2n-1)!} \prod_{1 \leq i < j \leq n} (a_j - a_i) \prod_{1 \leq i < j \leq n} (a_i + a_j), \quad (2.4)$$

where the empty products are equal to 1 by convention. The functions E and O were first introduced by Jockusch and Propp in [10] as the number of the so-called *anti-symmetric monotone triangles*, and the functions \bar{E} and \bar{O} were first introduced by the author in [16] as the tiling numbers of a family of regions called *quartered Aztec rectangles*.

Given a Douglas region $\mathcal{D} := \mathcal{D}_a(\mathbf{d}) = \mathcal{D}_a(d_1, d_2, \dots, d_k)$ that admits the southwest-to-northeast symmetry axis α . It is easy to see that we must have $d_i = d_{k-i+1}$, k is odd, and α is *not* a drawn-in diagonal (i.e., all the cells running along α are squares). We label the squares passed by α as follows. If the symmetry center of \mathcal{D} stays inside one of these squares, we call this square the *central cell*, and label it by 0. Next we label the two squares closest to the center by 1, we label the two squares that are second closest to the center by 2, and so on (see Figure 2.2). A cell of \mathcal{D} is said to be *regular* if it is either a black square or a black triangle pointing away from α . We define the *height* $h(\mathcal{D})$ of \mathcal{D} to be the number of rows of regular cells above α or passed by α . By the symmetry, $h(\mathcal{D})$ is also the number of rows of regular cells below α or passed by α . The number of regular cells which is on or above α is denoted by $\mathcal{C}(\mathcal{D})$, and we usually call it the *number of upper regular cells*. The number $w(\mathcal{D})$ of squares passed through by α is called the *width* of \mathcal{D} . We call a row of an odd number of black triangles pointing toward α and above α a *singular row*. The number of singular rows $\tau(\mathcal{D})$ is called the *defect* of \mathcal{D} . For example the left region in Figure 2.2 has respectively the height, the number of upper regular cells, the width, and the defect 5, 63, 12, 0; the region on the right of the figure has these parameters 5, 41, 5, 1, respectively.

We remove all squares having labels in a subset \mathcal{S} of $\{0, 1, 2, \dots, \lfloor \frac{w(\mathcal{D})}{2} \rfloor\}$ along α . Denote by the resulting region by $\mathcal{D}_a(\mathbf{d}; \mathcal{S})$ (see Figure 2.2 for examples; the black squares indicate the ones that have been removed). Assume that the complement of \mathcal{S} is $\{i_1, i_2, \dots, i_k\}$, for $1 \leq i_1 < i_2 < \dots < i_k \leq \lfloor \frac{w(\mathcal{D})}{2} \rfloor$. We define $\mathcal{O} = \mathcal{O}_{\mathcal{D}} := \{i_j : j \text{ is odd}\}$ and $\mathcal{E} = \mathcal{E}_{\mathcal{D}} := \{i_j : j \text{ is even}\}$.

²From now on, we use the words “*triangle(s)*” and “*square(s)*” to mean “*triangular cell(s)*” and “*square cell(s)*”, respectively.

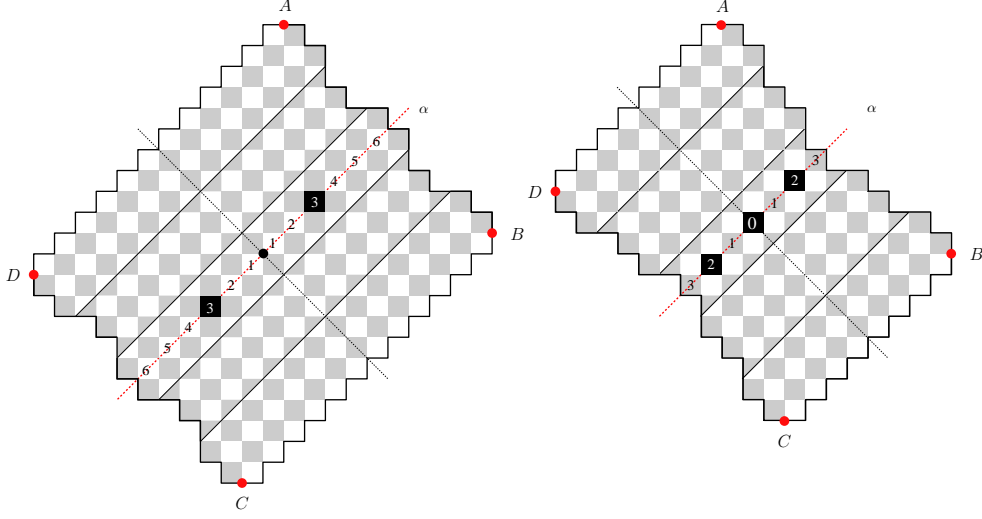


Figure 2.2: The Douglas regions with holes: $\mathcal{D}_{12}(4, 4, 4, 4, 4; \{3\})$ (left) and $\mathcal{D}_8(4, 5, 4, 5, 4; \{2\})$ (right).

We notice that if $\mathcal{D}_a(\mathbf{d}; \mathcal{S})$ admits a tiling, then the number of squares removed equals $|w(\mathcal{D}) - 2h(\mathcal{D})|$ if α passes white squares, and equals $|w(\mathcal{D}) - 2h(\mathcal{D}) + 1|$ otherwise. Moreover, in the latter case the central cell must be removed. The number of centrally symmetric tilings of the region $\mathcal{D}_a(\mathbf{d}; \mathcal{S})$ is given by the following theorem. In this paper we use the notation $M^*(\mathcal{R})$ for the number of centrally symmetric tilings of \mathcal{R} .

Theorem 2.1. *Given a positive a and a sequence of positive integers $\mathbf{d} = \{d_1\}_{i=1}^k$ so that the Douglas region $\mathcal{D} := \mathcal{D}_a(\mathbf{d})$ admits a southwest-to-northeast symmetry axis α and has the width $w = w(\mathcal{D})$, the height $h = h(\mathcal{D})$, the defect $\tau = \tau(\mathcal{D})$, and the number of upper regular cells $\mathcal{C} = \mathcal{C}(\mathcal{D})$. We remove all squares running along α with labels in $\mathcal{S} \subset \{0, 1, 2, \dots, \lfloor \frac{w}{2} \rfloor\}$ so that $|\mathcal{S}| = |w - 2h|$ if α passes white squares, and $|\mathcal{S}| = |w - 2h + 1|$, otherwise.*

(a) *Assume in addition that α passes white squares and $w \geq 2h$. Then*

$$M^*(\mathcal{D}_a(\mathbf{d}; \mathcal{S})) = 2^{\mathcal{C} - (w-1)h - \tau} E(\mathcal{O}) O(\mathcal{E}) \quad (2.5)$$

if w is even;

$$M^*(\mathcal{D}_a(\mathbf{d}; \mathcal{S})) = 2^{\mathcal{C} - (w-1)h - \tau - 1} \overline{E}(\mathcal{O}) \overline{O}(\mathcal{E}) \quad (2.6)$$

if h and w are odd;

$$M^*(\mathcal{D}_a(\mathbf{d}; \mathcal{S})) = 2^{\mathcal{C} - (w-1)h - \tau} \overline{E}(\mathcal{O}) \overline{O}(\mathcal{E}) \quad (2.7)$$

if h is even and w is odd.

(b) *Assume in addition that α passes black squares and $2h - 1 \geq w \geq h$. Then*

$$M^*(\mathcal{D}_a(\mathbf{d}; \mathcal{S})) = \frac{2^{\mathcal{C} - wh - \tau + \frac{w-1}{2}}}{(h-2)!} \overline{E}(\mathcal{S} \cup \mathcal{E}) \overline{O}(\mathcal{S} \cup \mathcal{O}) \quad (2.8)$$

if h is even and w is odd;

$$M^*(\mathcal{D}_a(\mathbf{d}; \mathcal{S})) = \frac{2^{\mathcal{C} - wh - \tau + \frac{w-1}{2}}}{(h-1)!} \overline{E}(\mathcal{S} \cup \mathcal{E}) \overline{O}(\mathcal{S} \cup \mathcal{O}) \quad (2.9)$$

if h and w are odd;

$$M^*(\mathcal{D}_a(\mathbf{d}; \mathcal{S})) = 2^{\mathcal{C} - (w+1)h - \tau + \frac{w}{2}} E(\mathcal{S} \cup \mathcal{E}) O(\mathcal{S} \cup \mathcal{O}) \quad (2.10)$$

if w is even.

We consider next the centrally symmetric tilings of a symmetric quasi-hexagon

$$\mathcal{H}_a(\mathbf{d}; \mathbf{d}) := \mathcal{H}_a(d_1, d_2, \dots, d_k; d_1, d_2, \dots, d_k).$$

Define the function

$$P(a, b, c) := \frac{(a-1)(2a-3)}{(b+a-1)(2b+2a-3)} \frac{\prod_{i=1}^{a-1} (b+i)^2 \prod_{i=1}^{a-2} (2b+2i-1)^2}{\prod_{i=1}^{a-1} i^2 \prod_{i=1}^{a-2} (2i-1)^2}. \quad (2.11)$$

This is exactly the number of self-complementary plane partitions fitting in the box $a \times b \times b$ (see Theorem 6.1 in [5]). The centrally symmetric tilings of a quasi-hexagon is given by the following theorem.

A *regular* cell of a quasi-hexagon \mathcal{H} is either a square or a triangle pointing away from the axis ℓ . We notice that a regular cells in a quasi-hexagon may be black or white (as opposed to being only black in the case of Douglas regions). Denote by $h_1(\mathcal{H})$ and $h_2(\mathcal{H})$ the number of rows of black regular cells above ℓ and the number rows of white regular cells below ℓ , respectively. We call $h_1(\mathcal{H})$ and $h_2(\mathcal{H})$ the *upper* and *lower heights* of \mathcal{H} . Denote $\mathcal{C}_1(\mathcal{H})$ and $\mathcal{C}_2(\mathcal{H})$ the number of black regular cells above ℓ and the number of white regular cells below ℓ , respectively. The *width* $w(\mathcal{H})$ of \mathcal{H} is the number of cells running along each side of ℓ . We still call a row of an odd number of black triangles pointing toward ℓ and above ℓ a *singular row* of \mathcal{H} . The number of singular rows $\tau(\mathcal{H})$ is also called the *defect* of \mathcal{H} .

Theorem 2.2. *Let a be a positive integer and $\mathbf{d} = (d_1, d_2, \dots, d_k)$ be a sequence of positive integers, so that for which the symmetric quasi-hexagon $\mathcal{H}_a(\mathbf{d}; \mathbf{d})$ has the heights $h = h_1 = h_2$ less than or equal to the width w . Assume that \mathcal{C} is the number of black regular cells above ℓ (and it is also the number of white regular cells below ℓ by the symmetry), and that τ is the defect of \mathcal{H} .*

(a) *If the h and w are even, then*

$$M^*(\mathcal{H}_a(\mathbf{d}; \mathbf{d})) = 2^{\mathcal{C} - \frac{h(2w-h+1)}{2} - \tau} P\left(\frac{h}{2}, \frac{h}{2}, \frac{w-h}{2}\right)^2. \quad (2.12)$$

(b) *If the h is even and w is odd, then*

$$M^*(\mathcal{H}_a(\mathbf{d}; \mathbf{d})) = 2^{\mathcal{C} - \frac{h(2w-h+1)}{2} - \tau} P\left(\frac{h}{2}, \frac{h}{2}, \frac{w-h-1}{2}\right) P\left(\frac{h}{2}, \frac{h}{2}, \frac{w-h+1}{2}\right). \quad (2.13)$$

(c) *If the h is odd and w is even, then*

$$M^*(\mathcal{H}_a(\mathbf{d}; \mathbf{d})) = 2^{\mathcal{C} - \frac{h(2w-h+1)}{2} - \tau} P\left(\frac{h-1}{2}, \frac{h+1}{2}, \frac{w-h}{2}\right)^2. \quad (2.14)$$

3 Preliminaries

This section shares several preliminary results and definitions with the prequels [13, 15] of the paper. The first result not reported in [13, 15] is Ciucu's Lemma 3.4.

A *perfect matching* of a graph G is a collection of edges such that each vertex of G is adjacent to exactly one edge in the collection. The tilings of a region \mathcal{R} can be naturally identified with the perfect matchings of its *dual graph* (i.e., the graph whose vertices are the cells of \mathcal{R} , and whose edges connect two cells precisely when they share an edge). In view of this, we denote the number of perfect matchings of a graph G by $M(G)$. More generally, if the edges of G have weights on them, $M(G)$ denotes the sum of the weights of all perfect matchings of G , where the *weight* of a perfect matching is the product of the weights on its constituent edges.

A *forced edge* of a graph G is an edge that is contained in every perfect matching of G . Let G be a weighted graph with weight function wt on its edges, and G' is obtained from G by removing forced

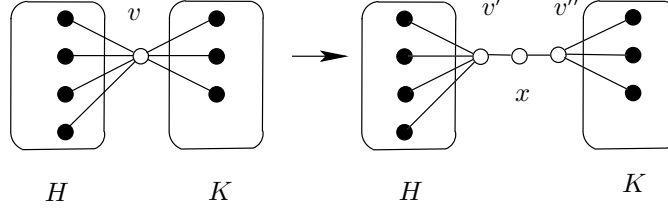


Figure 3.1: Vertex splitting.

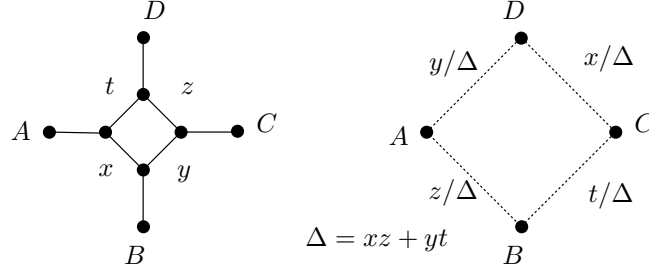


Figure 3.2: Urban renewal.

edges e_1, \dots, e_k , as well as the vertices incident to these edges³. Then one clearly has

$$M(G) = M(G') \prod_{i=1}^k \text{wt}(e_i). \quad (3.1)$$

We present next three basic preliminary results stated below.

Lemma 3.1 (Vertex-Splitting Lemma; Lemma 2.2 in [4]). *Let G be a graph, v be a vertex of it, and denote the set of neighbors of v by $N(v)$. For an arbitrary disjoint union $N(v) = H \cup K$, let G' be the graph obtained from $G \setminus v$ by including three new vertices v' , v'' and x so that $N(v') = H \cup \{x\}$, $N(v'') = K \cup \{x\}$, and $N(x) = \{v', v''\}$ (see Figure 3.1). Then $M(G) = M(G')$.*

Lemma 3.2 (Star Lemma; Lemma 3.2 in [13]). *Let G be a weighted graph, and let v be a vertex of G . Let G' be the graph obtained from G by multiplying the weights of all edges that are adjacent to v by $t > 0$. Then $M(G') = t M(G)$.*

Part (a) of the following result is a generalization due to Propp of the “urban renewal” trick first observed by Kuperberg. Parts (b) and (c) are due to Ciucu (see Lemma 2.6 in [5]).

Lemma 3.3 (Spider Lemma). *(a) Let G be a weighted graph containing the subgraph K shown on the left in Figure 3.2 (the labels indicate weights, unlabeled edges have weight 1). Suppose in addition that the four inner black vertices in the subgraph K , different from A, B, C, D , have no neighbors outside K . Let G' be the graph obtained from G by replacing K by the graph \bar{K} shown on right in Figure 3.3, where the dashed lines indicate new edges, weighted as shown. Then $M(G) = (xz + yt) M(G')$.*

(b) Consider the above local replacement operation when K and \bar{K} are graphs shown in Figure 3.3(a) with the indicated weights (in particular, K' has a new vertex D , that is incident only to A and C). Then $M(G) = 2 M(G')$.

(c) The statement of part (b) is also true when K and \bar{K} are the graphs indicated in Figure 3.3(b) (in this case G' has two new vertices C and D , they are adjacent only to one another and to B and A , respectively).

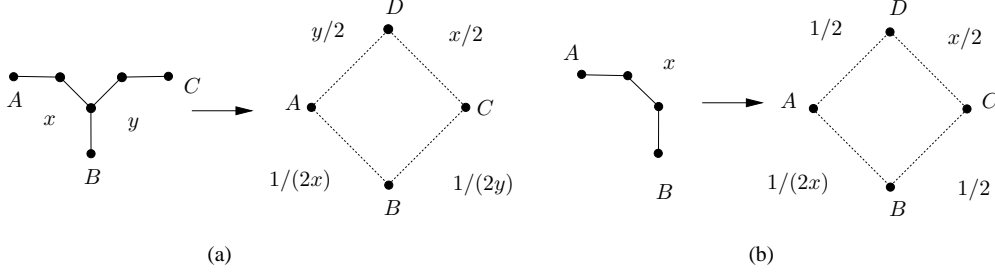


Figure 3.3: Two variants of the urban renewal.

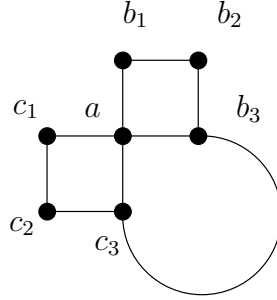


Figure 3.4: Illustrating Lemma 3.4.

We quote the following useful result lemma of Ciucu [2].

Lemma 3.4 (Lemma 4.2 in [2]). *Let G be a weighted graph having a 7-vertex subgraph H consisting of two 4-cycles that share a vertex. Let a, b_1, b_2, b_3 and a, c_1, c_2, c_3 be the vertices of the 4-cycles (listed in cyclic order) and suppose b_3 and c_3 are only the vertices of H with the neighbors outside H (see Figure 3.4). Let G' be the subgraph of G obtained by deleting b_1, b_2, c_1 and c_2 , weighted by restriction. Then if the product of weights of opposite edges in each 4-cycle of H is a constant, we have*

$$M(G) = 2wt(b_1, b_2)wt(c_1, c_2) M(G').$$

Next, we introduce a powerful in enumeration of perfect matchings of reflectively symmetric graphs. This was introduced by Ciucu [2].

Let G be a weighted planar bipartite graph that is symmetric about a horizontal line ℓ . Assume that the set of vertices lying on ℓ is a cut set of G (i.e., the removal of these vertices disconnects G). One readily sees that the number of vertices of G on ℓ must be even if G has perfect matchings, let $\eta(G)$ be half of this number. Let $a_1, b_1, a_2, b_2, \dots, a_{\eta(G)}, b_{\eta(G)}$ be the vertices lying on ℓ , as they occur from left to right. Color vertices of G by black or white so that any two adjacent vertices have opposite colors. Without loss of generality, we assume that a_1 is always colored white. Delete all edges above ℓ at all white a_i 's and black b_j 's, and delete all edges below ℓ at all black a_i 's and white b_j 's. Reduce the weight of each edge lying on ℓ by half; leave all other weights unchanged. Since the set of vertices of G on ℓ is a cut set, the graph obtained from the above cutting procedure has two disconnected parts, one above ℓ and one on below ℓ , denoted by G^+ and G^- , respectively (see Figure 3.5).

Theorem 3.5 (Ciucu's Factorization Theorem [2]). *Let G be a bipartite weighted symmetric graph separated by its symmetry axis. Then*

$$M(G) = 2^{\eta(G)} M(G^+) M(G^-). \quad (3.2)$$

³For the sake of simplicity, from now on, whenever we remove some forced edges, we remove also the vertices incident to them.

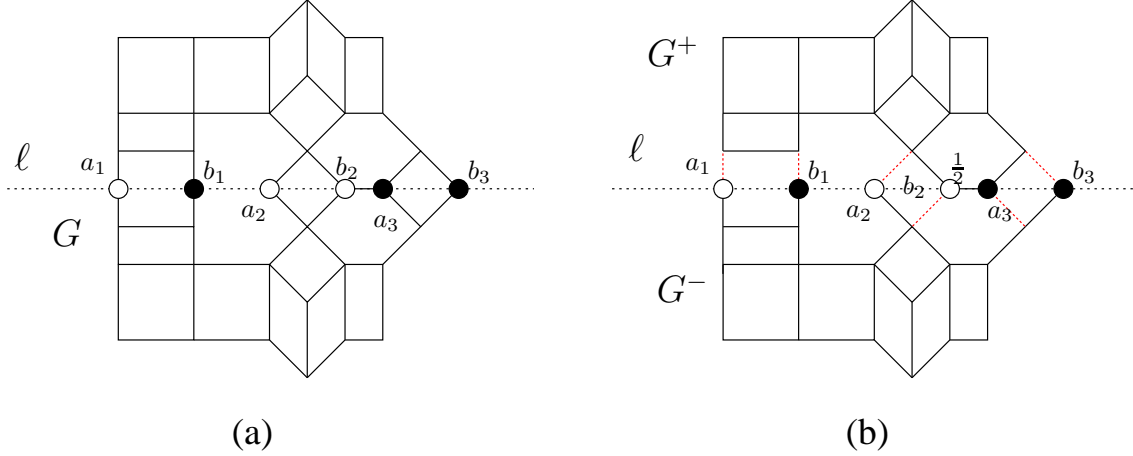


Figure 3.5: (a) A graph G with symmetric axis; (b) the resulting graph after the cutting procedure.

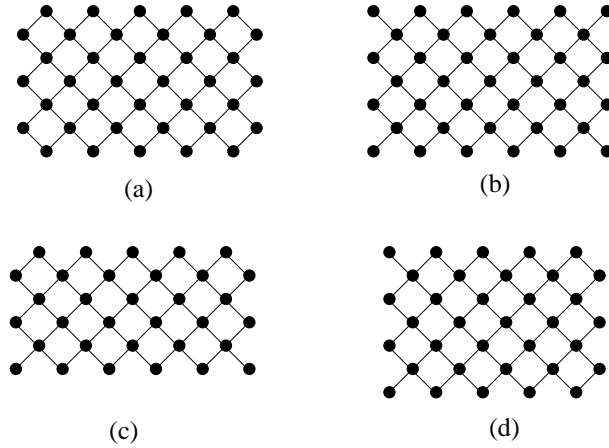


Figure 3.6: Four types of Aztec rectangle graphs.

Consider a $(2m+1) \times (2n+1)$ rectangular chessboard and suppose the corners are black. The *Aztec rectangle graph* $AR_{m,n}$ is the graph whose vertices are the white unit squares and whose edges connect precisely those pairs of white unit squares that are diagonally adjacent (see Figure 3.6(a) for $AR_{3,5}$). The *odd Aztec rectangle graph* $OR_{m,n}$ is the graph whose vertices are the black unit squares whose edges connect precisely those pairs of black unit squares that are diagonally adjacent (see Figure 3.6(b) for $OR_{3,5}$). If one removes the bottom row of the board B and applies the same procedure the definition of $AR_{m,n}$, the resulting graph is denoted by $AR_{m-\frac{1}{2},n}$, and called a *baseless Aztec rectangle* (see Figure 3.6(c) for $AR_{5/2,5}$). We also consider the graph $AR_{m,n-1/2}$ that is obtained from the Aztec rectangle $AR_{m,n}$ by removing all its leftmost vertices (see Figure 3.6(d) for $AR_{3,9/2}$).

It is worth noticing that when $n = m$, the Aztec rectangle graph $AR_{m,n}$ become the *Aztec diamond graph* AD_n . Elkies, Kuperberg, Larsen and Propp [8, 9] showed that the number of perfect matchings of AD_n is exactly $2^{n(n+1)/2}$. The Aztec rectangle graph $AR_{m,n}$ does *not* have perfect matchings in general, however, when certain vertices have been removed from one side of its, the perfect matchings are enumerated by a simple product formula (see e.g. Proposition 2.1 in [6]).

Next, we consider several variations of the Aztec rectangles ⁴ as follows.

⁴From now on we use the word “Aztec rectangle(s)” to mean “Aztec rectangle graphs”.

Label the vertices on the left side of the Aztec rectangle $AR_{m,n}$ from bottom up by $1, 2, 3, \dots, m$. Denote by $AR_{m,n}^o$ and $AR_{m,n}^e$ the graphs obtained from $AR_{m,n}$ by removing all odd-labeled and all even-labeled vertices, respectively (see Figures 5.5(b) and (d) for $AR_{6,5}^o$ and $AR_{5,5}^o$, and Figures 5.4(b) and (d) for $AR_{5,5}^e$ and $AR_{6,5}^e$). We call $AR_{m,n}^o$ and $AR_{m,n}^e$ the *odd-* and *even-trimmed versions* of $AR_{m,n}$, respectively.

Apply similarly process we obtain the odd- and even-trimmed versions of the graphs $OR_{m,n}$, $AR_{m-1/2,n}$, and $AR_{m,n-1/2}$. Figures 5.2(b) and (d) illustrate the graph $OR_{6,5}^o$ and $OR_{5,5}^o$; while the graphs $OR_{6,5}^e$ and $OR_{5,5}^e$ are shown in Figures 5.1(b) and (d). See Figures 5.7(b) and (d) for $AR_{5,9/2}^o$ and $AR_{6,9/2}^o$, and Figures 5.6(b) and (d) for $AR_{6,9/2}^e$ and $AR_{5,9/2}^e$. Finally, examples of $AR_{m,n}^o$ and $AR_{m,n}^e$ are illustrated in Figures 5.10(b) and (d) and in Figures 5.11(b) and (d), respectively.

Similar to the case of the Aztec rectangles, the above trimmed Aztec rectangles do not have perfect matchings in general, and we are interested in the case some bottom vertices of them have been removed.

Label the bottom vertices of $AR_{m,n}^e$, $AR_{m,n}^o$, $OR_{m,n}^e$, and $OR_{m,n}^o$ by $1, 2, \dots, n$ from left to right. For $0 \leq k \leq n$ and $1 \leq a_1 < a_2 < \dots < a_k \leq n$, define $AR_{m,n}^e(a_1, a_2, \dots, a_k)$ (resp., $AR_{m,n}^o(a_1, a_2, \dots, a_k)$) to be the graph obtained from $AR_{m,n}^e$ (resp., $AR_{m,n}^o$) by removing all bottom vertices, except for the ones at the positions a_1, a_2, \dots, a_k . Define $OR_{m,n}^e(a_1, a_2, \dots, a_k)$ (resp., $OR_{m,n}^o(a_1, a_2, \dots, a_k)$) to be the graph obtained from $OR_{m,n}^e$ (resp., $OR_{m,n}^o$) by removing the bottom vertices at the positions a_1, a_2, \dots, a_k .

Similarly, we label the bottom vertices of $AR_{m,n+1/2}^e$ and $AR_{m-1/2,n}^e$ by $0, 1, 2, \dots, n$ from left to right; and we also label the bottom vertices of $AR_{m,n+1/2}^o$ and $AR_{m-1/2,n}^o$ by $1, 2, \dots, n$. For $0 \leq k \leq n$ and $1 \leq a_1 < a_2 < \dots < a_k \leq n$, define $AR_{m,n+1/2}^e(a_1, a_2, \dots, a_k)$ (resp., $AR_{m,n+1/2}^o(a_1, a_2, \dots, a_k)$) to be the graph obtained from $AR_{m,n+1/2}^e$ (resp., $AR_{m,n+1/2}^o$) by removing all bottom vertices, except for the ones at the positions a_1, a_2, \dots, a_k . The graph $AR_{m-1/2,n}^e(a_1, a_2, \dots, a_k)$ (resp., $AR_{m-1/2,n}^o(a_1, a_2, \dots, a_k)$) is the graph obtained from $AR_{m-1/2,n}^e$ (resp., $AR_{m-1/2,n}^o$) by removing the bottom vertices at the positions 0 and a_1, a_2, \dots, a_k (resp., at the positions a_1, a_2, \dots, a_k).

The author showed that perfect matchings of a trimmed Aztec rectangle are always enumerated by a simple product formula (see Theorems 1.2 and 1.3 in [16]; strictly speaking, our graphs here are the dual graphs of the regions in these theorems).

Theorem 3.6. *For any $1 \leq k < n$ and $1 \leq a_1 < a_2 < \dots < a_k \leq n$*

$$M(AR_{2k-1,n}^e(a_1, a_2, \dots, a_k)) = M(AR_{2k,n}^e(a_1, a_2, \dots, a_k)) = E(a_1, a_2, \dots, a_k), \quad (3.3)$$

$$M(AR_{2k,n}^o(a_1, a_2, \dots, a_k)) = M(AR_{2k+1,n}^o(a_1, a_2, \dots, a_k)) = O(a_1, a_2, \dots, a_k), \quad (3.4)$$

$$M(OR_{2k,n}^e(a_1, a_2, \dots, a_k)) = M(OR_{2k+1,n}^e(a_1, a_2, \dots, a_k)) = 2^{-k} O(a_1, a_2, \dots, a_k), \quad (3.5)$$

$$M(OR_{2k-1,n}^o(a_1, a_2, \dots, a_k)) = M(OR_{2k,n}^o(a_1, a_2, \dots, a_k)) = 2^{-k} E(a_1, a_2, \dots, a_k), \quad (3.6)$$

$$M(AR_{2k,n-1/2}^o(a_1, a_2, \dots, a_k)) = M(AR_{2k+1,n-1/2}^o(a_1, a_2, \dots, a_k)) = 2^k \overline{O}(a_1, a_2, \dots, a_k), \quad (3.7)$$

$$M(AR_{2k-1,n-1/2}^e(a_1, a_2, \dots, a_k)) = M(AR_{2k,n-1/2}^e(a_1, a_2, \dots, a_k)) = 2^{-k} \overline{E}(a_1, a_2, \dots, a_k), \quad (3.8)$$

$$M(AR_{2k-1/2,n}^o(a_1, a_2, \dots, a_k)) = M(AR_{2k+1/2,n}^o(a_1, a_2, \dots, a_k)) = \overline{O}(a_1, a_2, \dots, a_k), \quad (3.9)$$

and

$$M(AR_{2k+1/2,n}^e(a_1, a_2, \dots, a_k)) = M(AR_{2k+3/2,n}^e(a_1, a_2, \dots, a_k)) = \frac{1}{(2k)!} \overline{E}(a_1, a_2, \dots, a_k). \quad (3.10)$$

4 Centrally symmetric matchings of an Aztec rectangle with holes

In his Ph.D. thesis [22], Bo-Yin Yang proved a conjecture posed by Jockush on the number of centrally symmetric tilings of the Aztec diamond region. Ciucu reproved the result in [2] by using his own factorization Theorem 3.5 and a tiling enumeration of Jockush and Propp [10]. This is worth noticing that the author gave a new proof for this Jockush–Propp enumeration in [14], and also generalized it in [16]. In this section, we enumerate centrally symmetric perfect matchings of an Aztec rectangle with several vertices removed along the symmetry axis. Our result implies Ciucu and Yang’s previous work as a special case when the set of removed vertices is empty (and the Aztec rectangle becomes an Aztec diamond graph).

Consider an Aztec rectangle $AR_{m,n}$ with the horizontal symmetry axis ℓ and the vertical symmetry axis ℓ' . We label the vertices of $AR_{a,b}$ on ℓ as follows. If the symmetry center of the graph is a vertex on ℓ , then we label it by 0. Label two vertices that is closest to the center by 1, label the second closest vertices by 2, and so on. We remove several vertices so that the resulting graph still admits the vertical symmetry axis ℓ' . Denote by \mathcal{S} the label set of removed vertices, which are not the center; and denote by $AR_{m,n}(\mathcal{S})$ the resulting graph. Assume that $\{i_1, i_2, \dots, i_k\}$ is the label set of the vertices of $AR_{m,n}(\mathcal{S})$ on ℓ . It is easy to see that if a bipartite graph has perfect matchings, then it must have the same number of vertices in the two vertex classes. This implies that in any cases $|\mathcal{S}| = |m - n|$. Moreover, for even m the graph $AR_{m,n}(\mathcal{S})$ has perfect matchings only if $m \leq n$; for odd m the graph $AR_{m,n}(\mathcal{S})$ has perfect matchings only if $m \geq n$. In the latter case we also have $n \geq m/2$, since the number of removed vertices $m - n$ must be less than or equal to the number of vertices in ℓ . In particular, Ciucu showed that if m is even and $m \leq n$, then the number of perfect matchings of $AR_{m,n}(\mathcal{S})$ is given by a simple product formula (see Theorem 4.1 in [2]).

We are interested in the centrally symmetric perfect matchings of $AR_{m,n}(\mathcal{S})$, i.e. the perfect matchings which are invariant under the 180° rotation around the symmetry center of the graph. Denote by $M^*(G)$ the number of centrally perfect matchings a graph G . We separate the label set of the vertices of $AR_{m,n}(\mathcal{S})$ on ℓ into two subsets: $\mathcal{O} := \{i_j : j \text{ is odd}\}$ and $\mathcal{E} := \{i_j : j \text{ is even}\}$.

The number of centrally symmetric perfect matchings of an Aztec rectangle graph with ‘holes’ $AR_{m,n}(\mathcal{S})$ is given by simple products in the following theorem.

Theorem 4.1. (a) For any $n > m$ and $\mathcal{S} = \{s_1, s_2, \dots, s_{n-m}\}$

$$M^*(AR_{2m,2n}(\mathcal{S})) = 2^m E(\mathcal{O}) O(\mathcal{E}) \quad (4.1)$$

(b) For any $m > n > m/2$ and $\mathcal{S} = \{s_1, s_2, \dots, s_{m-n}\}$

$$M^*(AR_{2m-1,2n-1}(\mathcal{S})) = 2^{n-m} E(\mathcal{S} \cup \mathcal{E}) O(\mathcal{S} \cup \mathcal{O}) \quad (4.2)$$

(c) For any $m > n > m/2$ and $\mathcal{S} = \{s_1, s_2, \dots, s_{m-n-1}\}$

$$M^*(AR_{2m-1,2n}(\mathcal{S})) = \begin{cases} \frac{2^n}{(m-2)!} \overline{E}(\mathcal{S} \cup \mathcal{E}) \overline{O}(\mathcal{S} \cup \mathcal{O}) & \text{if } m \text{ is even;} \\ \frac{2^n}{(m-1)!} \overline{E}(\mathcal{S} \cup \mathcal{E}) \overline{O}(\mathcal{S} \cup \mathcal{O}) & \text{if } m \text{ is odd;} \end{cases} \quad (4.3)$$

(d) For any $n > m$ and $\mathcal{S} = \{s_1, s_2, \dots, s_{n-m-1}\}$

$$M^*(AR_{2m,2n-1}(\mathcal{S})) = \begin{cases} 2^{m-1} \overline{E}(\mathcal{O}) \overline{O}(\mathcal{E}) & \text{if } m \text{ is odd;} \\ 2^m \overline{E}(\mathcal{O}) \overline{O}(\mathcal{E}) & \text{if } m \text{ is even.} \end{cases} \quad (4.4)$$

Proof of Theorem 4.1. We only prove in detail part (a), as the other parts can be obtained in a completely analogous manner. We will use Ciucu’s Factorization Theorem 3.5 to show that the number of centrally symmetric perfect matchings of our graph is given by a certain product of the numbers of perfect matchings of two graphs in Theorem 3.6.

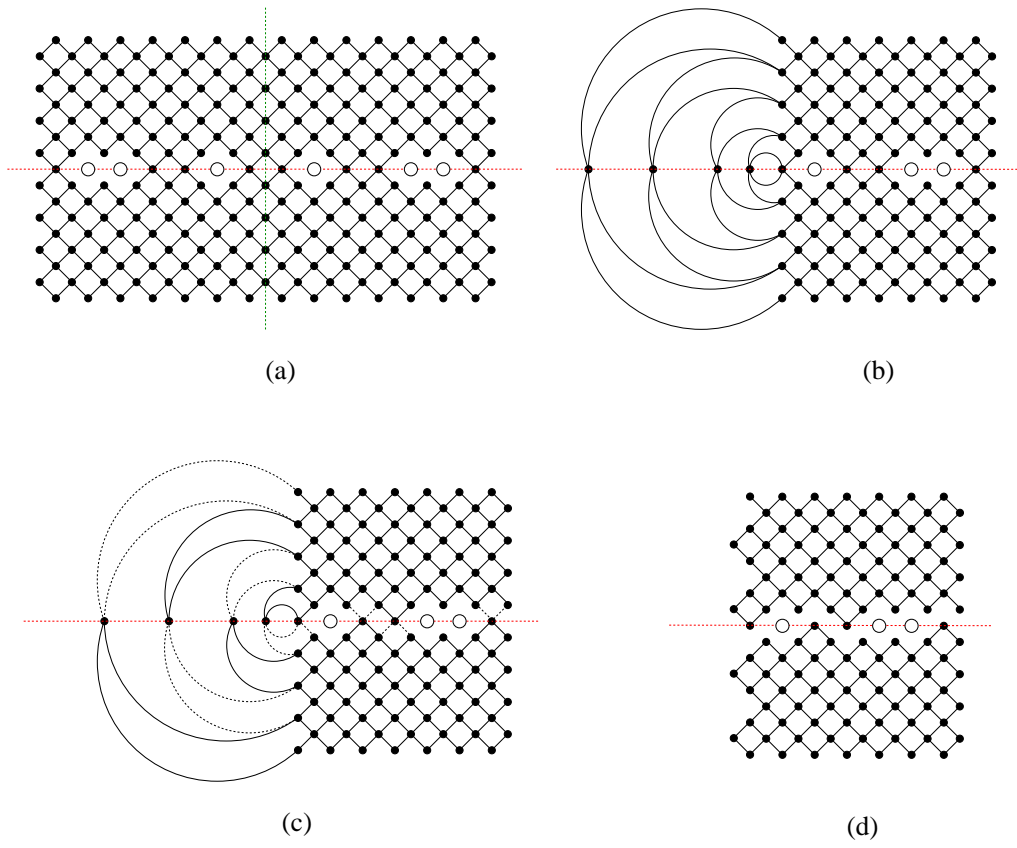


Figure 4.1: Illustrating of the proof of Theorem 4.1.

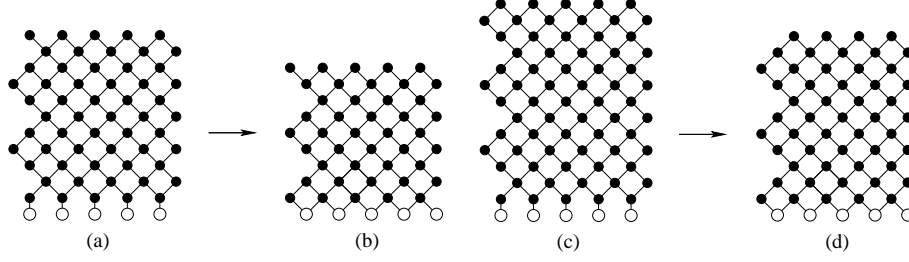


Figure 5.1: Illustrating the transformation in (5.1) of Lemma 5.1.

Consider the Aztec rectangle with holes $G = AR_{2m,2n}(\mathcal{S})$ with the horizontal and vertical symmetry axes ℓ and ℓ' (see Figure 4.1(a) for $AR_{8,14}(2,5,6)$). In this case $n \geq m$ and $|\mathcal{S}| = n - m$. Consider the subgraph H of G that is induced by vertices lying on ℓ' or staying on the right of ℓ' . Label the vertices of G on ℓ' which are staying above the horizontal axis ℓ by v_1, v_2, v_3, \dots from bottom to top; and label the vertices of G on ℓ' which are below ℓ by u_1, u_2, u_3, \dots from top to bottom.

It is readily to see that each centrally symmetric perfect matching μ of G is determined uniquely by its sub-matching μ' restricted to the edge set of H , i.e., $\mu' := \mu \cap E(H)$. On the other hand, by the symmetry of μ , exactly one of two vertices u_i and v_i is covered by μ' . Therefore, μ' corresponds to a perfect matching of the graph \tilde{H} obtained from H by identifying u_i and v_i , for any $i = 1, 2, 3, \dots$. This implies that the centrally symmetric perfect matchings of G are in bijection with the perfect matchings of \tilde{H} .

Moreover, we can put the vertices in \tilde{H} which are obtained by identifying u_i and v_i on the horizontal axis ℓ , so that \tilde{H} has ℓ as its horizontal symmetry axis (see Figure 4.1(b)). By Factorization Theorem 3.5, we have

$$M(\tilde{H}) = 2^m M(\tilde{H}^+) M(\tilde{H}^-), \quad (4.5)$$

where \tilde{H} has exactly $2m$ vertices on ℓ (see the cutting procedure in Figures 4.1(c) and (d)).

For even m , we have \tilde{H}^+ is isomorphic to $AR_{m,n}^e(\mathcal{O})$ and \tilde{H}^- is isomorphic to $AR_{m,n}^o(\mathcal{E})$ (see Figure 4.1(d)), while \tilde{H}^+ is isomorphic to $AR_{m,n}^o(\mathcal{E})$ and \tilde{H}^- is isomorphic to $AR_{m,n}^e(\mathcal{O})$ when m is odd. Therefore, (4.1) follows from Theorem 3.6. This finishes our proof. \square

5 Symmetric tilings of generalized Douglas region

In the first part of this section, we present several new subgraph replacement rules that will be employed in the proof of Theorem 2.1.

The *connected sum* $G \# G'$ of two disjoint graphs G and G' along the ordered sets of vertices $\{v_1, \dots, v_n\} \subset V(G)$ and $\{v'_1, \dots, v'_n\} \subset V(G')$ is the graph obtained from G and G' by identifying vertices v_i and v'_i , for $i = 1, 2, \dots, n$.

In the next lemmas (Lemmas 5.1, 5.2, 5.3, and 5.4), we always assume that G is a graph, and $\{v_1, v_2, \dots, v_n\}$ is an ordered set of its vertices. Moreover, all connected sums act on G along $\{v_1, v_2, \dots, v_n\}$ and on other summands along their bottommost vertices ordered from left to right.

Lemma 5.1.

$$M(|AR_{m,n}^o \# G) = 2^{\lfloor \frac{m}{2} \rfloor} M(OR_{m,n}^e \# G) \quad (5.1)$$

and

$$M(|AR_{m,n}^e \# G) = 2^{\lfloor \frac{m+1}{2} \rfloor} M(OR_{m,n}^o \# G), \quad (5.2)$$

where $|AR_{m,n}^o$ and $|AR_{m,n}^e$ are the graphs obtained from $AR_{m,n}^o$ and $AR_{m,n}^e$ by appending n vertical edges to their bottommost vertices, respectively (see Figure 5.1 for examples of the ‘transformation’ in (5.1), and Figure 5.2 for examples of the transformation in (5.2)).

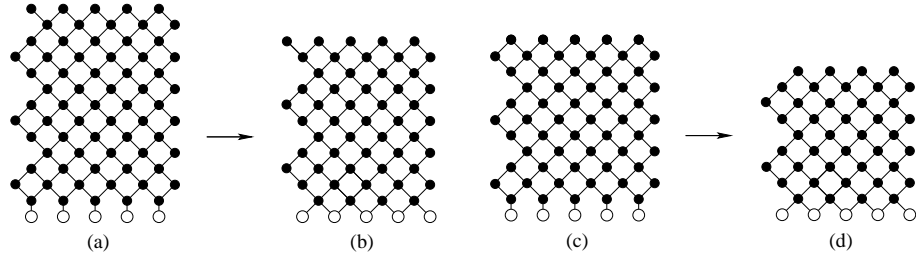


Figure 5.2: Illustrating the transformation in (5.2) of Lemma 5.1.

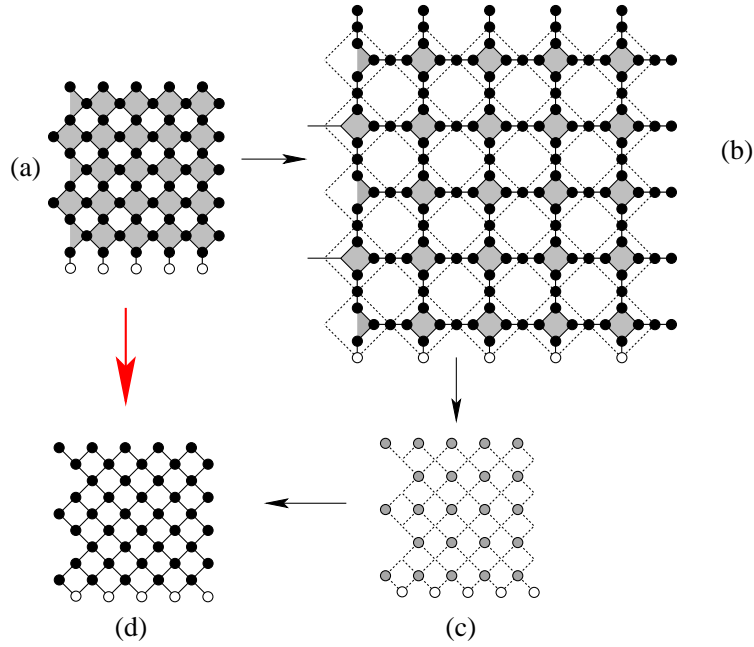


Figure 5.3: Illustration of the proof of Lemma 5.1.

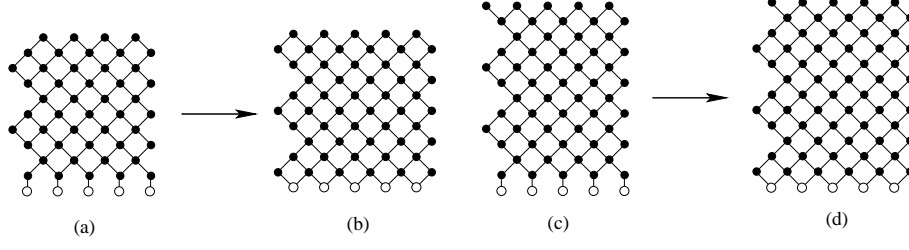


Figure 5.4: Illustrating the transformation in (5.4) of Lemma 5.2.

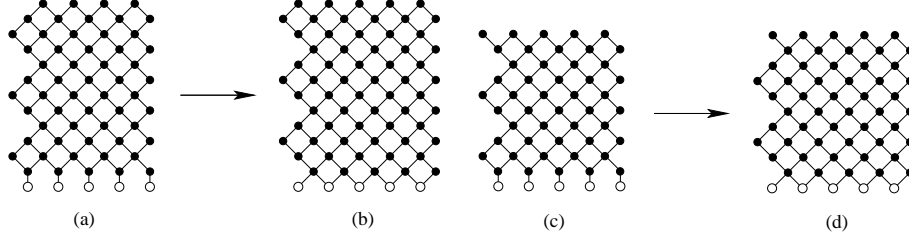


Figure 5.5: Illustrating the transformation in (5.5) of Lemma 5.2.

Proof. We only prove here the transformation in (5.1), based on Figure 5.3, for $m = n = 5$, as the transformation in (5.2) can be obtained in the same way.

First we apply the Vertex-splitting Lemma 3.1 to all vertices of $|AR_{m,n}^o \# G$ that are incident to a shaded diamond or a partial diamond as in Figure 5.3(a). We get the graph G_1 on Figure 5.3(b). Next, we apply Spider Lemma 3.3 around mn shaded diamonds and partial diamonds (the dotted edges have weight $1/2$), and remove all edges incident to a vertex of degree 1, which are forced. We obtain a weighted graph G_2 obtained from $OR_{m,n}^e \# G$ by assigning to each edge of $OR_{m,n}^e$ a weight $1/2$. Finally, we get back the graph $OR_{m,n}^e \# G$ by applying Star Lemma 3.2 with factor $t = 2$ at $mn - \lfloor \frac{m}{2} \rfloor$ shaded vertices as in Figure 5.3(c). By Lemmas 3.1, 3.2, and 3.3, we have

$$M(|AR_{m,n}^o \# G) = M(G_1) = 2^{mn} M(G_2) = 2^{mn} 2^{-(mn - \lfloor \frac{m}{2} \rfloor)} M(OR_{m,n}^e \# G), \quad (5.3)$$

which implies (5.1). \square

By applying the transformations in Lemma 5.1 (in reverse), and then Vertex-splitting Lemma 3.1, one can get the following transformations.

Lemma 5.2.

$$M(|OR_{m,n}^o \# G) = 2^{-\lfloor \frac{m+1}{2} \rfloor} M(AR_{m,n}^e \# G) \quad (5.4)$$

and

$$M(|OR_{m,n}^e \# G) = 2^{-\lfloor \frac{m}{2} \rfloor} M(AR_{m,n}^o \# G), \quad (5.5)$$

where $|OR_{m,n}^o$ and $|OR_{m,n}^e$ are the graphs obtained from $OR_{m,n}^o$ and $OR_{m,n}^e$ by appending n vertical edges to their bottommost vertices, respectively (Figure 5.4 shows the transformation in (5.4), and Figure 5.5 illustrates the transformation in (5.5)).

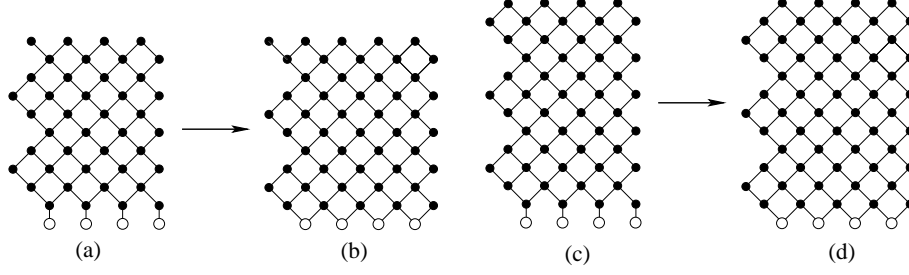


Figure 5.6: Illustrating the transformation in (5.6) of Lemma 5.3.

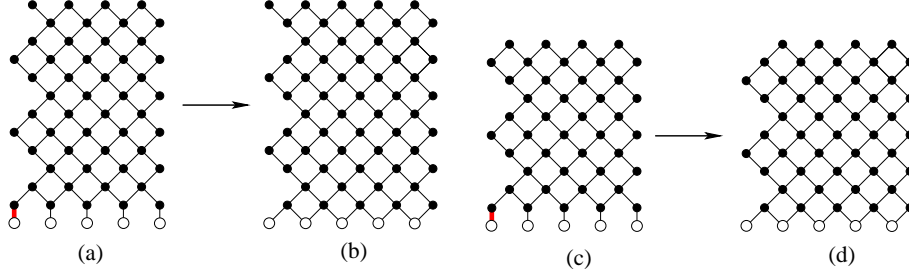


Figure 5.7: Illustrating the transformation in (5.7) of Lemma 5.3. The red bold edges at the lower-left corners of the graphs (a) and (c) are weighted by $1/2$.

By using Ciucu's Lemma 3.4 together with Lemmas 3.1–3.3, one gets the following lemma.

Lemma 5.3.

$$M(|AR_{m-1/2,n}^o \# G) = 2^{-\lfloor \frac{m}{2} \rfloor} M(AR_{m,n+1/2}^o \# G) \quad (5.6)$$

and

$$M(|AR_{m-1/2,n-1}^e \# G) = 2^{-\lfloor \frac{m+1}{2} \rfloor} M(AR_{m,n-1/2}^e \# G), \quad (5.7)$$

where $|AR_{m-1/2,n}^o$ is the graph obtained from $AR_{m-1/2,n}^o$ by appending n vertical edges to its bottommost vertices; and where $|AR_{m-1/2,n-1}^e$ is the graph obtained from $AR_{m-1/2,n-1}^e$ by appending n vertical edges to its bottommost vertices, the leftmost vertical edge is weighted $1/2$ (the transformation in (5.6) is shown in Figure 5.6, and the transformation in (5.7) is illustrated in Figure 5.7).

Proof. We only need to prove (5.6) for even m , and the case of odd m follows from the even case by removing the southeast-to-northwest forced edges on the top of $|AR_{m-1/2,n}^o$ and $AR_{m,n+1/2}^o$.

Our proof is illustrated in Figure 5.8, for $m = 4$ and $n = 4$.

First, apply Vertex-splitting Lemma 3.1 to the vertices in $|AR_{m-1/2,n}^o \# G$ that are incident to a shaded diamond or a partial diamond (see Figure 5.8(a) and (b)). Second, apply suitable replacement in Spider Lemma 3.3 around mn shaded diamonds and partial diamonds. Third, apply Lemma 3.4 to remove $\frac{m}{2}$ 7-vertex subgraph consisting of two shaded 4-cycles (see Figure 5.8(c); the dotted edges are weighted by $1/2$). Finally, apply the Star Lemma 3.2 with factor $t = 2$ to all $m(n+1)$ shaded vertices as in Figure 5.8(c). The resulting graph is exactly $AR_{m,n+1/2}^o \# G$. By Lemmas 3.1, 3.2, 3.3, and 3.4, we obtain

$$M(|AR_{m-1/2,n}^o \# G) = 2^{m(n+1)} 2^{-\frac{m}{2}} 2^{-m(n+1)} M(AR_{m,n+1/2}^o \# G), \quad (5.8)$$

which implies (5.6).

Next, we show the proof of (5.7) for odd m , the case of even m follows from the odd case by removing southeast-to-northwest forced edges on the top of $|AR_{m-1/2,n-1}^e$ and $AR_{m,n-1/2}^e$. Our proof is shown in Figure 5.9, for $m = 5$ and $n = 4$. We apply Vertex-splitting Lemma 3.1 to the vertices in $|AR_{m-1/2,n}^e \# G$

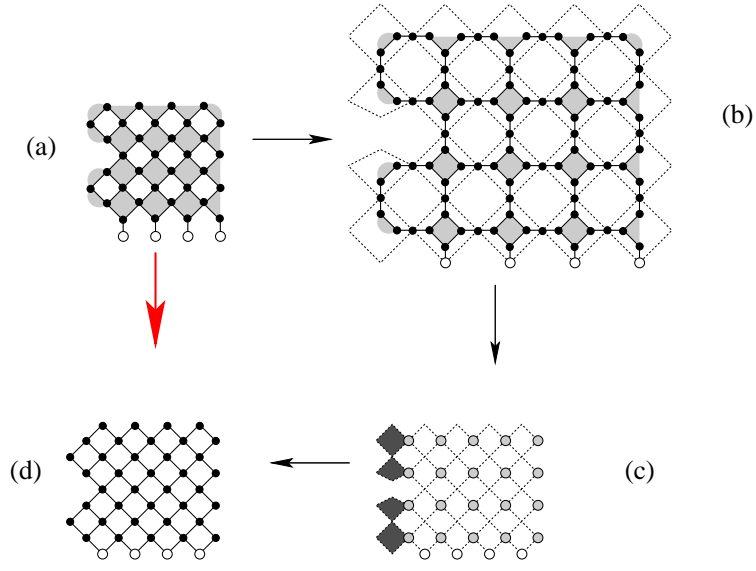


Figure 5.8: Illustrating the proof of (5.6) in Lemma 5.3.

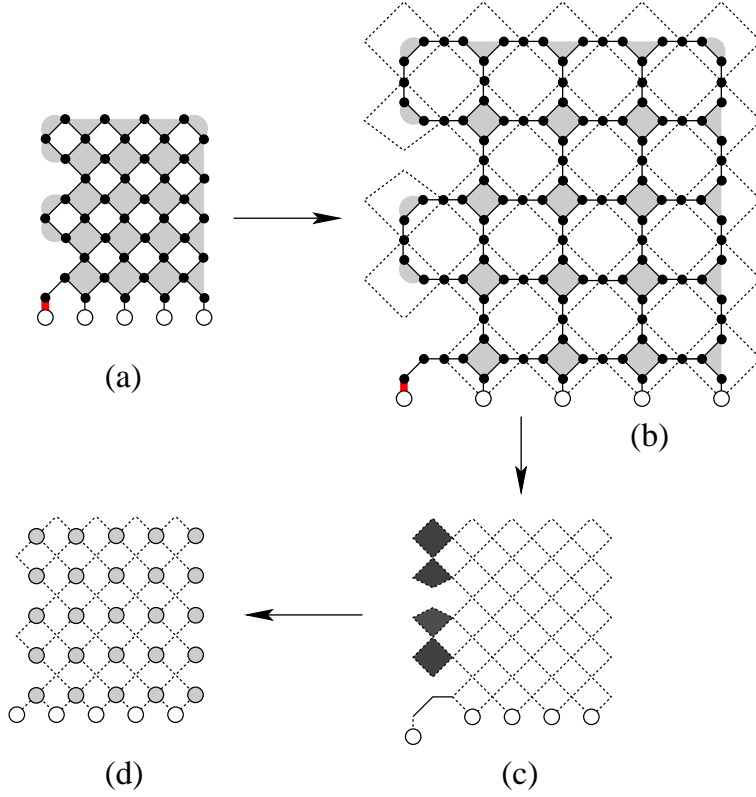


Figure 5.9: Illustrating the proof of (5.7) in Lemma 5.3.

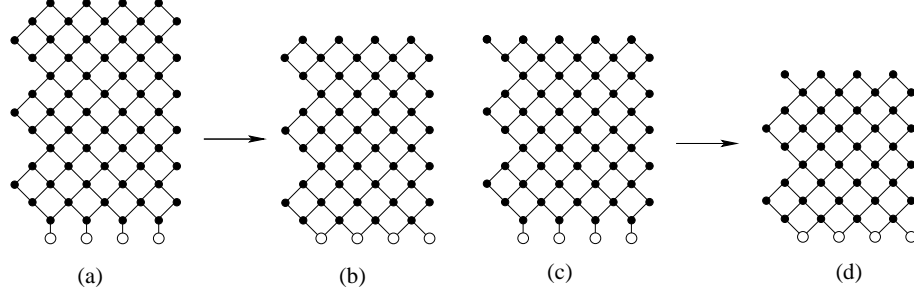


Figure 5.10: Illustrating the transformation in (5.10) of Lemma 5.4

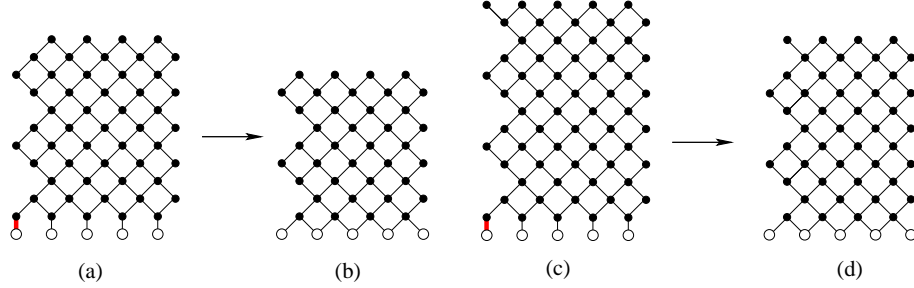


Figure 5.11: Illustrating the transformation in (5.11) of Lemma 5.4. Red edge has weight $1/2$.

incident to a shaded diamond or partial diamond as in Figures 5.9(a) and (b). Then apply Spider Lemma 3.3 to $m(n+1) - 1$ shaded diamonds and partial diamonds. Next, we apply Lemma 3.4 to remove $\frac{m-1}{2}$ subgraphs consisting of two shaded 4-cycles (see Figure 5.9(c); the dotted edges have weight $1/2$), and apply Vertex-splitting Lemma 3.1 (in reverse) to eliminate the two solid edges in the resulting graph. Finally, apply Star Lemma 3.2 (for the factor $t = 2$) to all $m(n+1)$ shaded vertices. This way, we obtain the graph $AR_{m,n-1/2}^e \# G$ on the right-hand side of (5.7). By Lemmas 3.1, 3.2, 3.3, and 3.4, we get

$$M(|AR_{m,n-1/2,n}^e \# G) = 2^{m(n+1)-1} 2^{-\frac{m-1}{2}} 2^{-m(n+1)} M(AR_{m,n+1/2}^e \# G), \quad (5.9)$$

which yields (5.7). \square

Similar to Lemma 5.3, we have the following lemma. The proof of the next lemma is essentially the same as that of Lemma 5.3, and will be omitted.

Lemma 5.4.

$$M(|AR_{m,n+1/2}^o \# G) = 2^{\lfloor \frac{m}{2} \rfloor} M(AR_{m-1/2,n}^o \# G), \quad (5.10)$$

and

$$M(|AR_{m,n-1/2}^e \# G) = 2^{\lfloor \frac{m+1}{2} \rfloor - 1} M(AR_{m-1/2,n-1}^e \# G), \quad (5.11)$$

where $|AR_{m,n+1/2}^o$ is the graph obtained from $AR_{m,n+1/2}^o$ by appending n vertical edges to its bottommost vertices; and where $|AR_{m,n-1/2}^e$ is the graph obtained from $AR_{m,n-1/2}^e$ by appending n vertical edges to its bottommost vertices, the leftmost vertical edge is weighted $1/2$ (the transformation in (5.10) is shown in Figure 5.10, and the transformation in (5.11) is illustrated in Figure 5.11).

We are now ready to prove Theorem 2.1.

Proof of Theorem 2.1. We only show in detail the proof for the case when α passes white squares and w is even, as the other cases can be obtained in the same manner.

We recall that α is not a drawn-in diagonal, and that k is odd in this case.

Let Q be any graph with the vertical and horizontal symmetry axes ℓ' and ℓ . We define the *orbit graph* $\text{Ob}(Q)$ of Q similarly to the proof of Theorem 4.1. In particular, we consider the subgraph H of Q that is induced by the vertices lying on the vertical axis ℓ' or staying on the right of ℓ' . The orbit graph $\text{Ob}(Q)$ of Q is the graph obtained by identifying two vertices of H on ℓ' that have the same distance to the symmetry center \mathbf{O} , so that the new vertices in $\text{Ob}(Q)$ on the ℓ (i.e. $\text{Ob}(Q)$ also has the horizontal symmetry axis ℓ). There is always a bijection between the centrally symmetric perfect matchings of G and the perfect matchings of its orbit graph $\text{Ob}(Q)$, i.e.

$$M^*(Q) = M(\text{Ob}(Q)).$$

Consider the dual graph G of the region $\mathcal{D}_a(\mathbf{d}; \mathcal{S})$ (rotated 45°). Its orbit graph $\text{Ob}(G)$ is illustrated in Figure 5.12. By Factorization Theorem 3.5, we have

$$M(\text{Ob}(G)) = 2^{\eta(\text{Ob}(G))} M(\text{Ob}(G)^+) M(\text{Ob}(G)^-), \quad (5.12)$$

where $\eta(\text{Ob}(G))$ is half of the number of vertices of $\text{Ob}(G)$ on its horizontal symmetry axis, and where the two component graphs $\text{Ob}(G)^+$ and $\text{Ob}(G)^-$ are illustrated in Figure 5.13.

By Theorem 3.6, we only need to show that

$$M^*(\mathcal{D}_a(\mathbf{d}; \mathcal{S})) = M(\text{Ob}(G)) = 2^{c-wh-\tau} M^*(AR_{2h,w}(\mathcal{S})). \quad (5.13)$$

The $k-1$ drawn-in diagonals divide the region $\mathcal{D}_a(\mathbf{d}; \mathcal{S})$ into k parts, called *layers*. We prove (5.13) by induction on the number of layers k (recall that k is odd by the symmetry of the Douglas region) of $\mathcal{D} = \mathcal{D}_a(d_1, d_2, \dots, d_k; \mathcal{S})$.

If $k=1$, then the dual graph of $\mathcal{D}_a(\mathbf{d}; \mathcal{S})$ is exactly $AR_{2h,w}(\mathcal{S})$, and (5.13) is a trivial identity. Assume that (5.13) is true for all ‘holey’ Douglas regions having less than k layers, $k \geq 3$, we need to show that (5.13) also holds for any holey Douglas region with k layers $\mathcal{D} = \mathcal{D}_a(d_1, d_2, \dots, d_k; \mathcal{S})$.

There are four cases to distinguish, based on the parities of d_1 and a .

Case 1. d_1 and a are even.

Define a new holey Douglas region \mathcal{D}' by

$$\mathcal{D}' := \mathcal{D}_{a-1}(d_1 + d_2 - 1, d_3, d_4, \dots, d_{k-2}, d_{k-1} + d_k - 1; \mathcal{S}) \text{ for } k \geq 5,$$

and

$$\mathcal{D}' := \mathcal{D}_{a-1}(d_1 + d_2 + d_3 - 2; \mathcal{S}) \text{ for } k = 3.$$

Denote by G' the dual graph of \mathcal{D}' .

By Factorization Theorem, we have

$$M(\text{Ob}(G')) = 2^{\eta(\text{Ob}(G'))} M(\text{Ob}(G')^+) M(\text{Ob}(G')^-), \quad (5.14)$$

where $\eta(\text{Ob}(G'))$ is half number of the vertices of $\text{Ob}(G')$ on the symmetry axis (see Figures 5.14(e) and (f)).

Assume that $d_1/2 = 2q$. Apply the transformation (5.2) in Lemma 5.1 to the top part of $\text{Ob}(G)^+$, that corresponds to the first layer of the region \mathcal{D} , we get the lower component graph $\text{Ob}(G')^-$ of the orbit graph $\text{Ob}(G')$ of G' , and obtain

$$M(\text{Ob}(G)^+) = 2^q M(\text{Ob}(G')^-). \quad (5.15)$$

This process is illustrated in Figures 5.14(a) and (b).

Similarly, we apply the transformation in (5.1) of Lemma 5.1 to the bottom part of $\text{Ob}(G)^-$, that corresponds to the bottom layer of \mathcal{D} , we get the upper component graph $\text{Ob}(G')^+$ of the orbit graph $\text{Ob}(G')$ of G' , and obtain

$$M(\text{Ob}(G)^-) = 2^q M(\text{Ob}(G')^+). \quad (5.16)$$

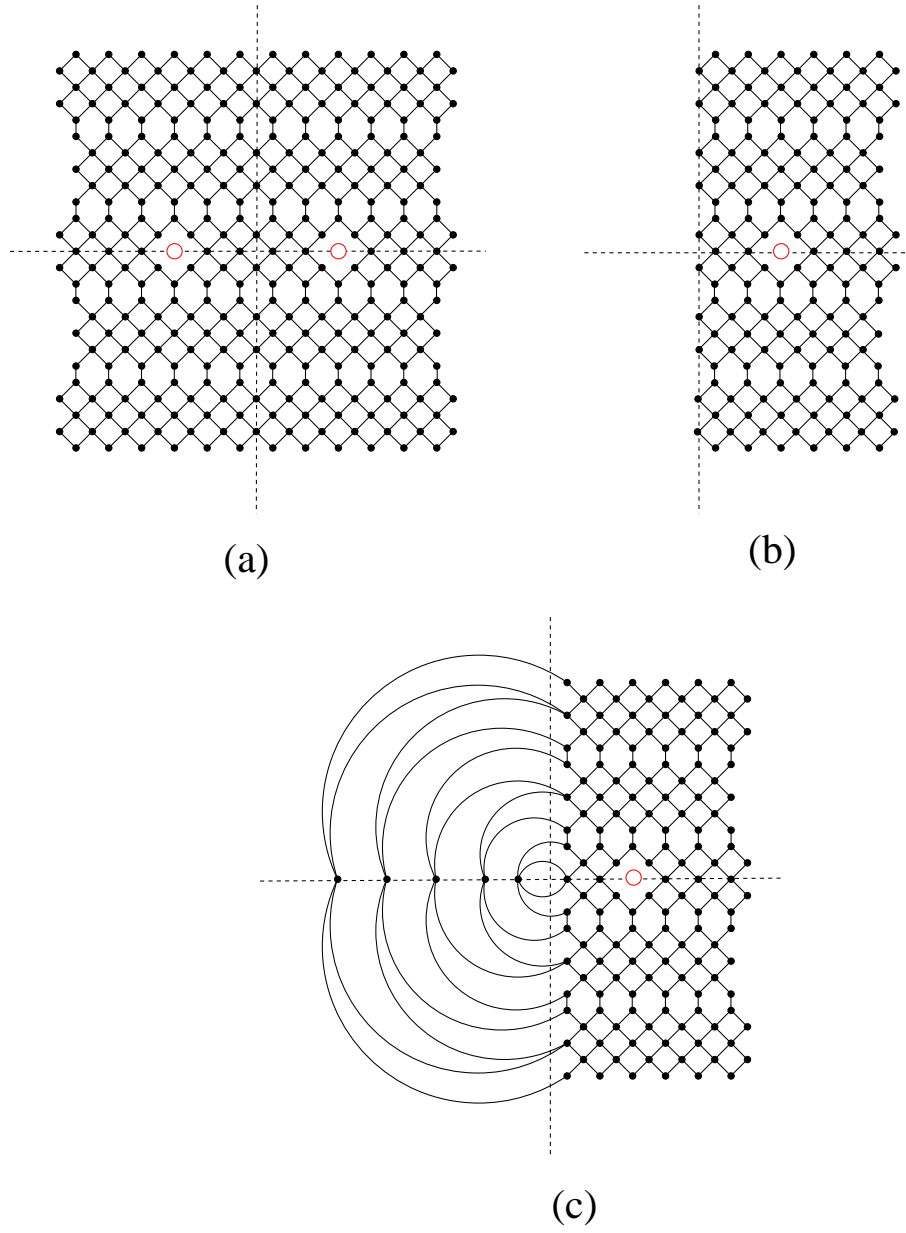


Figure 5.12: The dual graph of the holey Douglas region $\mathcal{D}_{12}(4, 4, 4, 4, 4; \{3\})$ and its orbit graph.

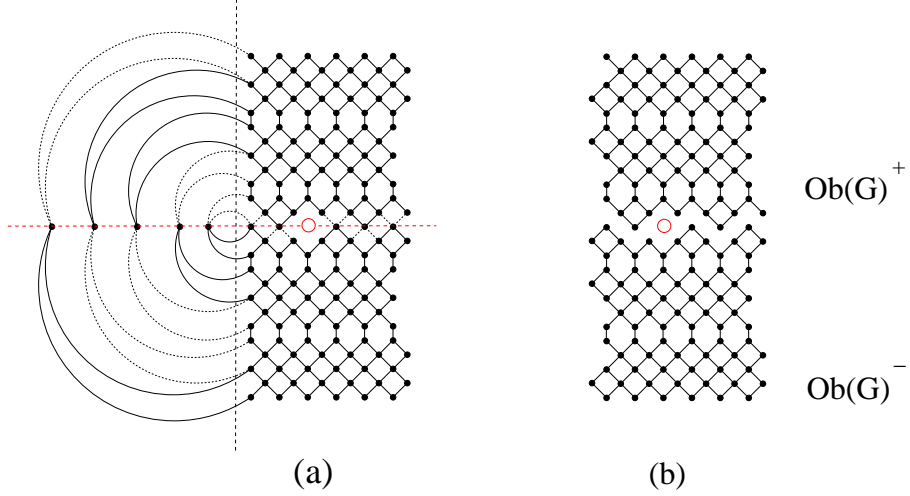


Figure 5.13: Separating the orbit graph of $\mathcal{D}_{12}(4, 4, 4, 4, 4; \{3\})$ into two component graphs.

This process is shown in Figures 5.14(c) and (d).

Multiply the two above equalities, we get

$$M(\text{Ob}(G)^+) M(\text{Ob}(G)^-) = 2^{2q} M(\text{Ob}(G')^+) M(\text{Ob}(G')^-). \quad (5.17)$$

By (5.12) and (5.14), we obtain

$$M(\text{Ob}(G)) = 2^{2q+\eta(\text{Ob}(G))-\eta(\text{Ob}(G'))} M(\text{Ob}(G')). \quad (5.18)$$

Since we are assuming that α passes white squares, the number of squares removed from α is $w - 2h$. It means that, the number vertices of G on ℓ is $2h$. Moreover, it is easy to see that the number of vertices of G running along the vertical symmetry axis ℓ' is also $2h$. Thus, $\eta(\text{Ob}(G)) = h$. Similarly, $\eta(\text{Ob}(G')) = h'$, where h' is the height of \mathcal{D}' .

One readily sees that \mathcal{D} and \mathcal{D}' have the same height, so $\eta(\text{Ob}(G)) = \eta(\text{Ob}(G'))$ in this case. It means that (5.18) can be simplified to

$$M(\text{Ob}(G)) = 2^{2q} M(\text{Ob}(G')). \quad (5.19)$$

Similarly, if $d_1/2 = 2q + 1$, then we apply transformation (5.2) in Lemma 5.1 to the top part of $\text{Ob}(G)^+$, we get the graph $\text{Ob}(G')^-$ and

$$M(\text{Ob}(G)^+) = 2^q M(\text{Ob}(G')^-). \quad (5.20)$$

Next, we apply the transformation (5.1) to the bottom part of $\text{Ob}(G)^-$, we get the graph $\text{Ob}(G')^+$ and

$$M(\text{Ob}(G)^-) = 2^{q+1} M(\text{Ob}(G')^+). \quad (5.21)$$

Therefore, similar to (5.19), we have

$$M(\text{Ob}(G)) = 2^{2q+1} M(\text{Ob}(G')). \quad (5.22)$$

By (5.19) and (5.22), we always have

$$M(\text{Ob}(G)) = 2^{d_1/2} M(\text{Ob}(G')). \quad (5.23)$$

Assume that α' is the axis of \mathcal{D}' . Denote by w', \mathcal{C}', τ' the width, the number of black regular cells above α' , and the defect of \mathcal{D}' , respectively. One readily sees that $w = w'$, $\tau = \tau'$, and

$$\mathcal{C} - \mathcal{C}' = d_1/2(a + 1) - d_1/2a = d_1/2.$$

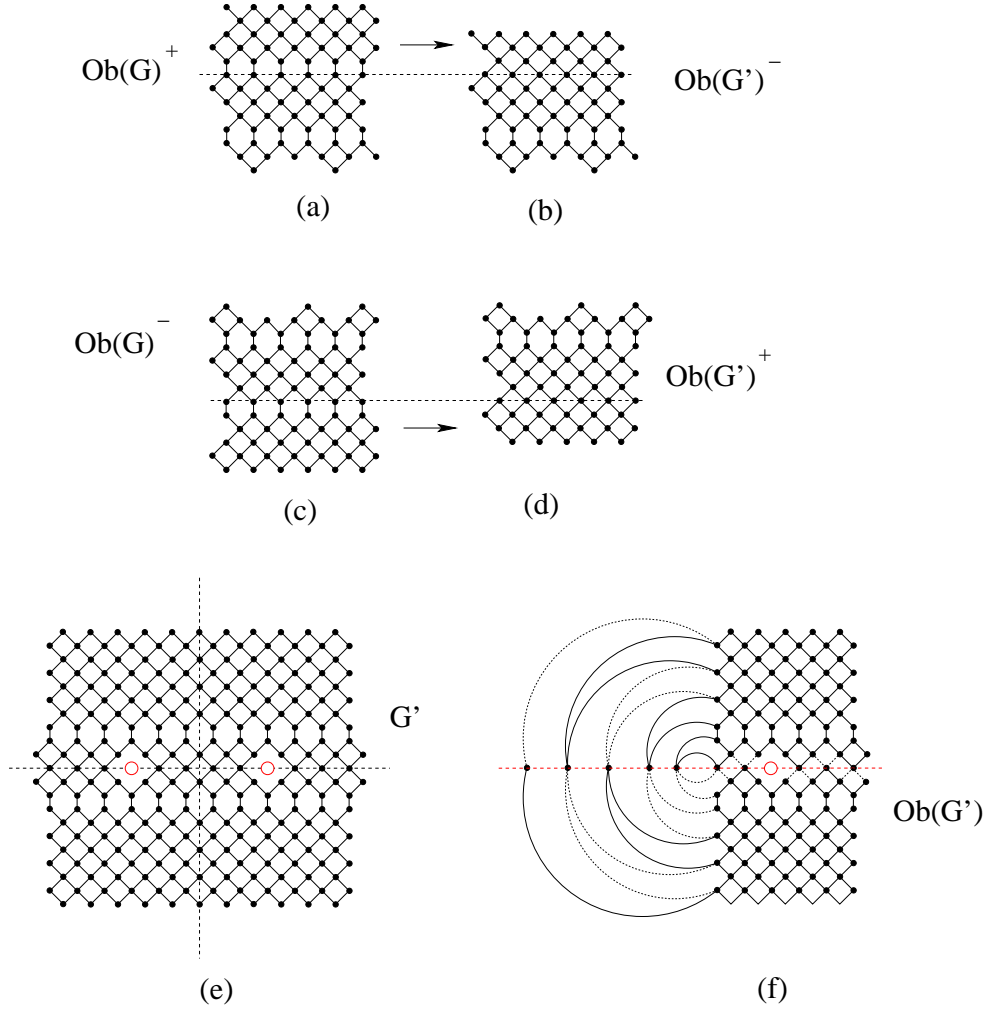


Figure 5.14: Transforming the orbit graph of $\mathcal{D} = \mathcal{D}_{12}(4, 4, 4, 4, 4; \{3\})$ into the orbit graph of $\mathcal{D}' = \mathcal{D}_{12}(7, 4, 7; \{3\})$.

By induction hypothesis for the region \mathcal{D}' , that has only $k - 2$ layers:

$$M(\text{Ob}(G)) = 2^{C' - w'h' - \tau'} M^*(AR_{2h', w'}(\mathcal{S})) \quad (5.24)$$

$$= 2^{C - d_1/2 - wh - \tau} M^*(AR_{2h, w}(\mathcal{S})), \quad (5.25)$$

and (5.13) follows from (5.23).

Case 2. d_1 and a odd.

Define a new holey Douglas region \mathcal{D}'' as

$$\mathcal{D}'' := \mathcal{D}_{a+1}(d_1 + d_2 + 1, d_3, d_4, \dots, d_{k-2}, d_{k-1} + d_k + 1) \text{ for } k \geq 5,$$

and

$$\mathcal{D}'' := \mathcal{D}_{a+1}(d_1 + d_2 + d_3 + 2) \text{ for } k = 3.$$

Denote by G'' its dual graph.

Do similarly to Case 1, we now apply the transformations in Lemma 5.2 to the top part of $\text{Ob}(G)^+$ or the bottom part of $\text{Ob}(G)^-$. If $(d_1 + 1)/2 = 2q$, then we get

$$M(\text{Ob}(G)) = 2^{-2q + \eta(\text{Ob}(G)) - \eta(\text{Ob}(G''))} M(\text{Ob}(G'')), \quad (5.26)$$

and if $(d_1 + 1)/2 = 2q + 1$, then

$$M(\text{Ob}(G)) = 2^{-2q-1 + \eta(\text{Ob}(G)) - \eta(\text{Ob}(G''))} M(\text{Ob}(G'')), \quad (5.27)$$

where $\eta(\text{Ob}(G''))$ is half of the number of vertices of G'' on its horizontal symmetry axis.

Moreover, \mathcal{D} and \mathcal{D}'' also have the same height, so $\eta(\text{Ob}(G)) = \eta(\text{Ob}(G''))$. Then thus, we always have in this case

$$M(\text{Ob}(G)) = 2^{-(d_1+1)/2} M(\text{Ob}(G'')). \quad (5.28)$$

Denote by w'', h'', C'', τ'' the width, the height, the number of black regular cells in the upper part, and the defect of \mathcal{D}'' , respectively. We also have $h = h'', w = w'', \tau = \tau''$. Moreover,

$$C - C'' = (d_1 + 1)/2(a + 1) - (d_1 + 1)/2(a + 2) = -(d_1 + 1)/2.$$

Thus (5.13) follows from (5.28) and the induction hypothesis for \mathcal{D}'' .

Case 3. d_1 is odd and a is even.

Apply the same procedure as in Case 1 and Case 2 by using suitable transformations in Lemma 5.3 to the top part of $\text{Ob}(G)^+$ or the bottom part of $\text{Ob}(G)^-$. We also get

$$M(\text{Ob}(G)) = 2^{-(d_1+1)/2} M(\text{Ob}(G'')), \quad (5.29)$$

where G'' is the dual graph of the region \mathcal{D}'' defined as in Case 2. Similarly to Case 2, we have (5.13).

Case 4. d_1 is even and a is odd.

Again, we apply the same procedure as that in the three previous cases by using suitable transformations in Lemma 5.4 to the top part of $\text{Ob}(G)^+$ or the bottom part of $\text{Ob}(G)^-$.

If $d_1/2 = 2q$, we get

$$M(\text{Ob}(G)) = 2^{2q-1 + \eta(\text{Ob}(G)) - \eta(\text{Ob}(G'))} M(\text{Ob}(G')); \quad (5.30)$$

and if $d_1/2 = 2q + 1$, then

$$M(\text{Ob}(G)) = 2^{2q + \eta(\text{Ob}(G)) - \eta(\text{Ob}(G'))} M(\text{Ob}(G')), \quad (5.31)$$

where G' is the dual graph of the region \mathcal{D}' defined as in Case 1. Then thus, we always have

$$M(\text{Ob}(G)) = 2^{d_1/2-1} M(\text{Ob}(G')). \quad (5.32)$$

Similarly, to Case 1, we have $w' = w$, $h = h'$, and $\mathcal{C} - \mathcal{C}' = d_1/2$. However, in this case $\tau' = \tau - 1$, since we have a singular row staying right below the first layer of \mathcal{D} , but it does not appear in \mathcal{D}' . Thus, by induction hypothesis for \mathcal{D}' and (5.32), we have

$$M(\text{Ob}(G)) = 2^{d_1/2-1} 2^{\mathcal{C}'-h'w'-\tau'} M^*(AR_{2h',w'}(\mathcal{S})) \quad (5.33)$$

$$= 2^{d_1/2-1} 2^{\mathcal{C}-d_1/2-hw-(\tau-1)} M^*(AR_{2h,w}(\mathcal{S})). \quad (5.34)$$

Then (5.13) follows. \square

6 Symmetric tilings of Quasi-hexagons

In this section, we use our transformations in Lemmas 5.1–5.4 to prove Theorem 2.2.

Proof of Theorem 2.2. There are two cases to distinguish based on the color of the up-pointing triangles running along the axis of $H_a(\mathbf{d}; \mathbf{d})$. We consider first the case when these triangles are black.

We consider the dual graph G of the region $\mathcal{H} = \mathcal{H}_a(\mathbf{d}; \mathbf{d})$ (rotated 45°) with the horizontal and vertical axes ℓ and ℓ' . Similar to the proof of Theorem 2.1, the number of centrally symmetric tilings of \mathcal{H} is equal to the number of centrally symmetric perfect matching of its dual graph G , the latter in turn equals the number of perfect matchings of its orbit graph $\text{Ob}(G)$.

The region \mathcal{H} has k layers above the axis, called the *upper layers*. Next, we prove by induction on the number of upper layers of \mathcal{H} that

Claim 6.1.

$$M(\text{Ob}(G)) = 2^{\mathcal{C}-hw-\tau} M(\text{Ob}(\overline{G})), \quad (6.1)$$

where \overline{G} is the dual graph of the region $\overline{\mathcal{H}} := \mathcal{H}_{w-1}(2h-1; 2h-1)$.

Proof. If $k = 1$, then (6.1) is a trivial identity, since $\mathcal{H} = \overline{\mathcal{H}}$. Assume that (6.1) holds for any symmetric quasi-hexagon with less than k ($k \geq 2$) upper layers, we need to show that the equality holds also for any symmetric quasi-hexagon $\mathcal{H} = \mathcal{H}_a(d_1, \dots, d_k; d_1, \dots, d_k)$.

We use similar arguments to that in the proof of Theorem 2.1. In particular, we transform the orbit graph of $\mathcal{H}_a(\mathbf{d}; \mathbf{d})$ into the orbit of a symmetric quasi-hexagon that has less layers by using the suitable transformations in Lemmas 5.1–5.4.

We only show in details the proof for the case when a and d_1 are even, as the other cases can be obtained similarly.

Similar to the Theorem 7.1 in [2], we notice that we cannot apply the Factorization Theorem 3.5 directly here, since the vertices of the orbit graph $\text{Ob}(G)$ on ℓ , $\{a_1, b_1, a_2, b_2, \dots, a_{\eta(\text{Ob}(G))}, b_{\eta(\text{Ob}(G))}\}$, do *not* form a cut set. However, the Lemma 2.1 in [2] still applies, it means that all $2^{\eta(G)}$ graphs, that are obtained from $\text{Ob}(G)$ by cutting edges from above or below each of a_i 's, have the same number of perfect matchings. We now consider a cutting procedure at the vertices a_i 's as follows. First, we color the vertices of $\text{Ob}(G)$ inductively from left to right: color a_1 by white, then color the next vertex the same color as its left one if there is not an edge connecting them, otherwise we use the opposite color (see Figure 6.1(b)). Assume that Q^* is the graph obtained from $\text{Ob}(G)$ by cutting above all white a_i 's and below all black a_i 's. We will show in the next paragraph that all perfect matchings of Q^* have the white b_j 's matched upward, and black b_j 's matched downward.

Indeed, we consider the collection \mathfrak{G} of $2^{\eta(G)}$ graphs obtained from Q^* by cutting at all edges incident to b_j 's from above or below. The matching set of Q^* is in bijection to disjoint union of matching sets of the members in \mathfrak{G} . Recall that if a bipartite admits a perfect matching, then its vertex classes must have the same size. All members Q of \mathfrak{G} are bipartite graphs, and it easy to check that its two vertex classes have the same size only if Q is obtained from cutting below all white b_j 's and above all black b_j 's.

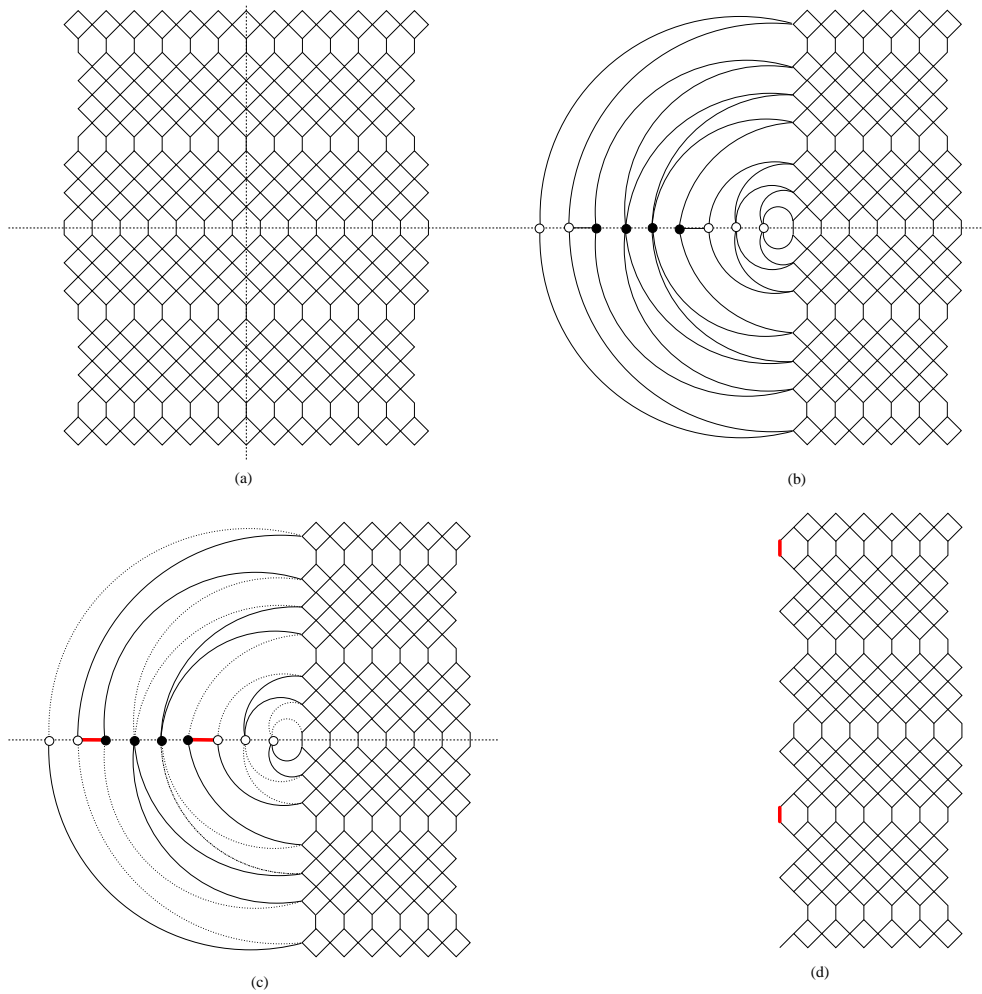


Figure 6.1: Obtaining the graph $Si(G)$ from G . The dotted edges indicate the ones cut off. The bold edges have weight $1/2$.

Now denote by $Si(G)$ the graph obtained from the orbit graph $Ob(G)$ of G by cutting above all white a_i 's and black b_j 's, and below all black a_i 's and white b_j 's (illustrated in in Figure 6.1(c)). Moreover, $Si(G)$ can be deformed into a weighted subgraph of G as in Figure 6.1(c)). Then we get

$$M(Ob(G)) = 2^{\eta(G)} M(Si(G)). \quad (6.2)$$

Apply the transformations in Lemma 5.1 to the top and bottom parts of $Si(G)$, that corresponding to the top and bottom layers of \mathcal{H} , we get the graph isomorphic to $Si(G')$, where G' is the dual graph of the quasi-hexagon \mathcal{H}' defined by

$$\mathcal{H}' := \mathcal{H}_{a-1}(d_1 + d_2 - 1; d_3, \dots, d_k; d_1 + d_2 - 1; d_3, \dots, d_k),$$

ans where $Si(G')$ is the graph obtained from the orbit graph $Ob(G')$ of G' by the same cutting procedure as in the case of G . We obtain

$$\begin{aligned} M(Ob(G)) &= 2^{\eta(G)} Si(G) \\ &= 2^{\eta(G)} 2^{d_1/2} Si(G') \\ &= 2^{d_1/2} 2^{\eta(G')} Si(G') \\ &= 2^{d_1/2} M(Ob(G')). \end{aligned} \quad (6.3)$$

By (6.3), the induction hypothesis, and explicit calculation of the statistics of the region \mathcal{H}' , we obtain

$$M(Ob(G)) = 2^{d_1/2} 2^{C' - h'w' - \tau'} M(Ob(\overline{G})) \quad (6.4)$$

$$= 2^{d_1/2} 2^{C - d_1/2 - hw - \tau} M(Ob(\overline{G})), \quad (6.5)$$

where C', h', w', τ' refer to \mathcal{H}' corresponding to their unprimed counterparts in \mathcal{H} . Then (6.1) follows, and this finishes the proof of our claim. \square

Consider the dual graph G'' of the symmetric quasi-hexagon region

$$\mathcal{H}'' := \mathcal{H}_{w-h}(\mathbf{1}^h; \mathbf{1}^h),$$

where all distances d_1, d_2, \dots, d_k are 1, and where $k = h$. \mathcal{H}'' is exactly the semi-regular hexagon of side-lengths $h, w-h, h, h, w-h, h$ on the triangular lattice. Apply the claim above to the orbit graph $Ob(G'')$ of G'' , we have

$$M(Ob(G'')) = 2^{-h(h-1)/2} M(Ob(\overline{G})). \quad (6.6)$$

Thus, by (6.1) and (6.6), we obtain

$$M(Ob(G)) = 2^{C-h(2w-h+1)/2-\tau} M(Ob(G'')). \quad (6.7)$$

The number of perfect matchings of $Ob(G'')$ is given by Ciucu's Theorem 7.1 in [5], and our theorem follows in the case when the triangles right above the axis ℓ are black .

Next, we consider the case where the triangles right above ℓ are white. Similarly, we can prove that by induction on k that

$$M(Ob(G)) = 2^{C-h(w+1)-\tau} M(Ob(\overline{\overline{G}})) \quad (6.8)$$

$$= 2^{C-h(w+1)-\tau} 2^{\eta(\overline{\overline{G}})} M(Si(\overline{\overline{G}})), \quad (6.9)$$

where $\overline{\overline{G}}$ is the dual graph of the region $\overline{\overline{\mathcal{H}}} := \mathcal{H}_w(2h; 2h)$, and $Si(\overline{\overline{G}})$ is the graph obtained from the orbit graph $Ob(\overline{\overline{G}})$ of $\overline{\overline{G}}$ by applying the cutting procedure in the previous case.

Next, we apply the Vertex-splitting Lemma 3.1 to all vertices at the bottom of the upper part of $Si(\overline{\overline{G}})$ (see Figure 6.2(b)), and apply the suitable transformations in Lemmas 5.1–5.4, we transform $Si(\overline{\overline{G}})$ into $Si(\overline{G})$, where \overline{G} is the dual graph of $\mathcal{H}_{w-1}(2h-1; 2h-1)$ as defined in the previous case (see Figure 6.2(c)). Then this case follows from the case we treated before. \square

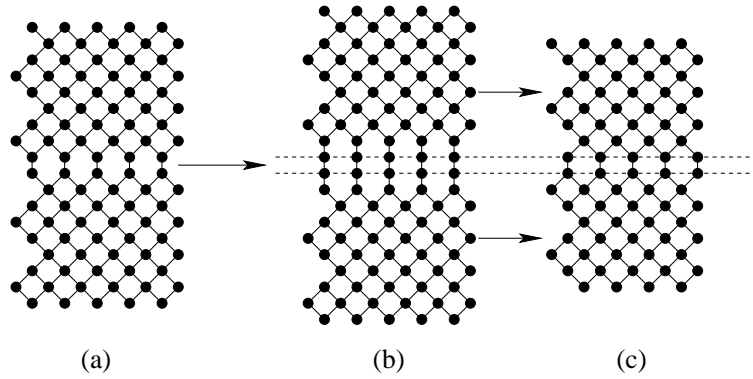


Figure 6.2: Transforming $Si(\overline{\overline{G}})$ into $Si(\overline{G})$.

References

- [1] L. Carlitz and R. Stanley, *Branching and partitions*, Proc. Amer. Math. Soc. **53**(1) (1975), 246–249.
- [2] M. Ciucu, *Enumeration of perfect matchings in graphs with reflective symmetry*, J. Combin. Theory Ser. A **77** (1997), 67–97.
- [3] M. Ciucu, *A complementation theorem for perfect matchings of graphs having a cellular completion*, J. Combin. Theory Ser. A **81** (1998), 34–68.
- [4] M. Ciucu, *Perfect matchings and applications*, COE Lecture Note, No. 26 (Math-for-Industry Lecture Note Series). Kyushu University, Faculty of Mathematics, Fukuoka (2000), 1–67.
- [5] M. Ciucu and C. Krattenthaler, *Plane partitions II: $5\frac{1}{2}$ Symmetric Classes*, Adv. Stud. Pure Math. **28** (2000), 83–103.
- [6] H. Cohn, M. Larsen, and J. Propp, *The Shape of a Typical Boxed Plane Partition*, New York J. Math. **4** (1998), 137–165.
- [7] C. Douglas, *An illustrative study of the enumeration of tilings: Conjecture discovery and proof techniques*, 1996. Available at <http://citeseerx.ist.psu.edu/viewdoc/summary?doi=10.1.1.44.8060>
- [8] N. Elkies, G. Kuperberg, M.Larsen, and J. Propp, *Alternating-sign matrices and domino tilings (Part I)*, J. Algebraic Combin. **1** (1992): 111–132.
- [9] N. Elkies, G. Kuperberg, M.Larsen, and J. Propp, *Alternating-sign matrices and domino tilings (Part II)*, J. Algebraic Combin. **1** (1992): 219–234.
- [10] W. Jockusch and J. Propp, *Antisymmetric monotone triangles and domino tilings of quartered Aztec diamonds*, Unpublished work.
- [11] P. A. MacMahon, *Combinatory Analysis*, Cambridge Univ. Press, London, 1916, reprinted by Chelsea, New York, 1960.
- [12] P. A. MacMahon, *Partitions of numbers whose graphs possess symmetry*, Trans. Cambridge Philos. Soc. **17** (1899), 149–170.
- [13] T. Lai, *Enumeration of hybrid domino-lozenge tilings*, J. Combin. Theory Ser. A **122**(2014), 53–81.
- [14] T. Lai, *A simple proof for the number of tilings of quartered Aztec diamonds*, Electron. J. Combin., **21**(1) (2014), P1.6.
- [15] T. Lai, *Enumeration of hybrid domino-lozenge tilings II: Quasi-octagonal regions* (2014), Preprint: arXiv:1310.3332.
- [16] T. Lai, *Enumeration of tilings of quartered Aztec rectangles*, Electron. J. Combin. **21**(4) (2014), P4.46.

- [17] T. Lai, *A generalization of Aztec diamond theorem, part I*, Electron. J. Combin. **21**(1) (2014), P1.51.
- [18] T. Lai, *A generalization of Aztec diamond theorem, part II*, Discrete Math. **339**(3) (2016), 1172–1179.
- [19] J. Propp, *Enumeration of matchings: Problems and progress*, New Perspectives in Geometric Combinatorics, Cambridge University Press (1992), 255–291.
- [20] R. Stanley, *Symmetric plane partitions*, J. Combin. Theory Ser. A **43** (1986), 103–113.
- [21] R. Stanley, *Enumerative Combinatorics, Vol. 2*, Cambridge Univ. Press, 1999.
- [22] B.-Y. Yang, *Two enumeration problems about Aztec diamonds*, Ph.D. thesis, Department of Mathematics, Massachusetts Institute of Technology, MA, 1991.